NUREG/IA-0147

International Agreement Report

Assessment of RELAP5/MOD3.2 for Steam Condensation Experiments in the Presence of Noncondensibles in a Vertical Tube of PCCS

Prepared by
H. S. Park, H. C. No/KAIST
Y. S. Bang, K. W. Seul, H. J. Kim/KINS

Korea Advanced Institute of Science & Technology
373-1 Kuseong-Dong, Yusong-Ku
Taejon, Korea

Korea Institute of Nuclear Safety
P.O. Box 114
Yusong, Taejon
Korea 305-600

Office of Nuclear Regulatory Research
U.S. Nuclear Regulatory Commission
Washington, DC 20555-0001

September 1998

Prepared as part of
The Agreement on Research Participation and Technical Exchange under the
International Thermal-Hydraulic Code Assessment and Maintenance Program (CAMP)

Published by
U.S. Nuclear Regulatory Commission

AVAILABILITY NOTICE

Availability of Reference Materials Cited in NRC Publications

NRC publications in the NUREG series, NRC regulations, and *Title 10, Energy,* of the *Code of Federal Regulations,* may be purchased from one of the following sources:

1. The Superintendent of Documents
   U.S. Government Printing Office
   P.O. Box 37082
   Washington, DC 20402–9328
   <http://www.access.gpo.gov/su_docs>
   202–512–1800

2. The National Technical Information Service
   Springfield, VA 22161–0002
   <http://www.ntis.gov/ordernow>
   703–487–4650

The NUREG series comprises (1) technical and administrative reports, including those prepared for international agreements, (2) brochures, (3) proceedings of conferences and workshops, (4) adjudications and other issuances of the Commission and Atomic Safety and Licensing Boards, and (5) books.

A single copy of each NRC draft report is available free, to the extent of supply, upon written request as follows:

Address: Office of the Chief Information Officer
Reproduction and Distribution
Services Section
U.S. Nuclear Regulatory Commission
Washington, DC 20555–0001
E-mail: <GRW1@NRC.GOV>
Facsimile: 301–415–2289

A portion of NRC regulatory and technical information is available at NRC's World Wide Web site:

<http://www.nrc.gov>

All NRC documents released to the public are available for inspection or copying for a fee, in paper, microfiche, or, in some cases, diskette, from the Public Document Room (PDR):

NRC Public Document Room
2121 L Street, N.W., Lower Level
Washington, DC 20555–0001
<http://www.nrc.gov/NRC/PDR/pdr1.htm>
1–800–397–4209 or locally 202–634–3273

Microfiche of most NRC documents made publicly available since January 1981 may be found in the Local Public Document Rooms (LPDRs) located in the vicinity of nuclear power plants. The locations of the LPDRs may be obtained from the PDR (see previous paragraph) or through:

<http://www.nrc.gov/NRC/NUREGS/SR1350/V9/lpdr/html>

Publicly released documents include, to name a few, NUREG-series reports; *Federal Register* notices; applicant, licensee, and vendor documents and correspondence; NRC correspondence and internal memoranda; bulletins and information notices; inspection and investigation reports; licensee event reports; and Commission papers and their attachments.

Documents available from public and special technical libraries include all open literature items, such as books, journal articles, and transactions, *Federal Register* notices, Federal and State legislation, and congressional reports. Such documents as theses, dissertations, foreign reports and translations, and non-NRC conference proceedings may be purchased from their sponsoring organization.

Copies of industry codes and standards used in a substantive manner in the NRC regulatory process are maintained at the NRC Library, Two White Flint North, 11545 Rockville Pike, Rockville, MD 20852–2738. These standards are available in the library for reference use by the public. Codes and standards are usually copyrighted and may be purchased from the originating organization or, if they are American National Standards, from—

American National Standards Institute
11 West 42nd Street
New York, NY 10036–8002
<http://www.ansi.org>
212–642–4900

NUREG/IA-0147

International Agreement Report

Assessment of RELAP5/MOD3.2 for Steam Condensation Experiments in the Presence of Noncondensibles in a Vertical Tube of PCCS

Prepared by
H. S. Park, H. C. No/KAIST
Y. S. Bang, K. W. Seul, H. J. Kim/KINS

Korea Advanced Institute of Science & Technology
373-1 Kuseong-Dong, Yusong-Ku
Taejon, Korea

Korea Institute of Nuclear Safety
P.O. Box 114
Yusong, Taejon
Korea 305-600

Office of Nuclear Regulatory Research
U.S. Nuclear Regulatory Commission
Washington, DC 20555-0001

September 1998

Prepared as part of
The Agreement on Research Participation and Technical Exchange under the
International Thermal-Hydraulic Code Assessment and Maintenance Program (CAMP)

Published by
U.S. Nuclear Regulatory Commission

Assessment of RELAP5/MOD3.2 for Steam Condensation Experiments in the Presence of Noncondensables in a Vertical Tube of PCCS

Abstract

This report deals with the application of RELAP5/MOD3.2 to condensation experiments in the presence of noncondensable gases in a vertical tube of Passive Containment Cooling System. When steam-noncondensable gas mixture was injected into the vertical tube, steam was condensed on the inner surface of the condensing tube but the noncondensable gas greatly inhibited the condensation of the steam. As the scattering of previous experimental data was large, the present experimental apparatus was set up to get a reliable data on the condensation heat transfer coefficient of the steam-noncondensable gas mixture in a vertical tube. The experimental results show that the condensation heat transfer coefficient increases as the inlet steam-air mixture flow rate increases, the inlet air mass fraction decreases, and the inlet saturated steam temperature decreases. There are two wall film condensation models, the default model and the alternative model, in RELAP5/MOD3.2. After a condensation database was constructed, two models were assessed directly with the data of the database. The experimental apparatus was also modeled with RELAP5/MOD3.2, and simulations were performed for several sub-tests to be compared with the experimental results. The simulation results show that in overall sense the default model of RELAP5/MOD3.2 under-predicts the heat transfer coefficients, but that the alternative model of RELAP5/MOD3.2 over-predicts them throughout the condensing tube. Different from the modeling results of RELAP5/MOD3.1, the change in the number of the nodes for condensing tube has little influence on the simulation results of RELAP5/MOD3.2 both with the default and with the alternative model. From the sensitivity study of input parameters it is also shown that the effects of the coolant flow rate, the inlet coolant temperature and the vented mixture temperature are negligible, but that the effects of the inlet mixture flow rate, the inlet saturated steam temperature and the inlet air mass fraction are significant. Run statistics show that the grind time of the default model is always about 23% higher than that of the alternative model.

Contents

List of Tables

List of Figures

Executive Summary

The RELAP5/MOD3.2 code is assessed with steam condensation experiments in the presence of noncondensables in a vertical tube of PCCS.

CARR Passive reactor(CP-1300), a large passive PWR concepts which was developed at Center for Advanced Reactor Research(CARR), has a concrete containment and the final safety functions are achieved through passive systems such as accumulator, Core Makeup Tank(CMT), Secondary Condenser(SC), and Passive Containment Cooling System(PCCS). Two concepts using internal condensers or an external condensers are proposed as PCCSs of CP-1300. The main concern of PCCS with the external condenser is the degradation of condensation heat transfer due to the accumulation of the air inside the condensing tubes.

The best-estimate safety analysis code, RELAP5/MOD3.2, which was developed at Idaho National Engineering Laboratory(INEL) based on international cooperation, CAMP, organized by U.S. NRC, is used to analyze the transients and the LOCA of a nuclear power plant. However much uncertainties are known to exist in some heat transfer correlations of RELAP5/MOD3.2, especially in modeling the condensation phenomena with noncondensable gases in a vertical condensing tube which is applicable to the design of PCCS and SC. The experimental apparatus were set up to get reliable data on the condensation heat transfer coefficient of the steam-noncondensable gas mixture in a vertical tube.

The objective of the present work is to assess the analysis capability of the RELAP5/MOD3.2 code on the condensation of the steam-noncondensable gas mixture in a vertical tube. First of all, two wall film condensation models in RELAP5/MOD3.2, the default model and the alternative model, were assessed with the constructed database. Two wall film condensation models of RELAP5/MOD3.2 were also assessed extensively for several experiments simulating steam condensation in the presence of noncondensables in a vertical tube of PCCS.

The test facility was nodalized so as to be suitable for simulating the important experimental parameters, which is known to be important in condensation experiments. The base case calculations were executed, the results were compared with the experimental data, two wall film condensation models of RELAP5/MOD3.2 were compared each other, and the code

predictability on the condensation phenomena was discussed. Nodalization study was performed to investigate the effect of the divided node number in the test section. Sensitivity studies were performed to investigate the effects of input parameters on heat transfer characteristics. Run statistics of two simulation results with different condensation models were also compared.

From the studies, the followings are obtained:

- The experimental results show that the inlet steam-air mixture flow rate, the inlet air mass fraction, and the inlet saturated steam temperature have significant effects on condensation heat transfer. The condensation heat transfer coefficient increases as the inlet steam-air mixture flow rate increases, the inlet air mass fraction decreases, and the inlet saturated steam temperature decreases.

- Two wall film condensation models in RELAP5/MOD3.2 are directly assessed with the constructed condensation database. The default model under-predicts the experimental data for the low heat transfer coefficient range, but it over-predicts the experimental data for the high heat transfer coefficient range. In case of the alternative model, the predicted values are always higher than the experimental data.

- As base case calculations several experiments are simulated by RELAP5/MOD3.2 with both the default model and the alternative model. When two wall film condensation models are compared each other, the calculated air mass fraction from the default model is always lower than that of the alternative model, all the calculated temperatures from the default model decrease more slowly than those from the alternative model, and the calculated heat flux from the default model is always lower than that from the alternative model in the upper part of the condensing tube, and they are similar in the lower part.

- Those results also show that with low inlet mixture flow rate and high inlet air mass fraction the default model under-predicts the experimental heat transfer coefficient, but

that the alternative model over-predicts it. With high inlet mixture flow rate and low inlet air mass fraction, the default model predicts the experimental data well, but the alternative model still over-predicts it, especially in the middle of the test section.

- From the nodalization study of RELAP5/MOD3.2, the change in the number of the nodes for condensing tube has little influence on the simulation results of the condensation phenomena with RELAP5/MOD3.2.

- As a sensitivity study several input parameters are changed to show their effects on heat transfer characteristics. The simulation results show that the effects of the inlet steam-air mixture flow rate, the inlet air mass fraction, and the inlet saturated steam temperature are most influential in condensation experiments in the presence of non-condensable gas in a vertical tube. However the effects of the coolant flow rate, the inlet coolant temperature, and the vented mixture temperature are shown to be less influential.

- Run statistics show that the grind time of the default model is always higher than that of the alternative model and it is a little increased for both models when more volumes are included in RELAP5/MOD3.2 simulation. The required CPU time is the highest when the inlet mixture flow rate is the highest and both the inlet air mass fraction and the inlet saturated steam temperature are the lowest.

- As both the default model and the alternative model can not predict well the experimental data, it is needed to develop a new correlation for wall film condensation based on the experimental data produced over various operating ranges, and it can be applied as a new condensation model to simulate the condensation heat transfer of the steam-noncondensable gas mixture in a vertical tube.

Acknowledgment

This report was performed under the sponsorship of Korea Atomic Energy Research Institute(KAERI). Authors appreciate the KAERI for the financial support.

Chapter 1

Introduction

1.1 Background

CP-1300[1, 2], a next generation reactor which is a large passive pressurized water reactor concept, was developed conceptually by CARR. It adopts several passive engineered-safety-features such as accumulator, CMT, SC, and PCCS, which are investigated extensively[3, 4].

Two types of PCCS are proposed as the long term cooling methods of the concrete containment[5]. An internal condenser concept is the one and an external condenser concept is the other. The internal condenser concept utilizes the natural circulation of the PCCS pool water through the condenser tubes inside a containment, while the external condenser concept utilizes the condensation in condensing tubes, which are located in a water pool outside a containment. Figure 1.1 is the conceptual design of the PCCS with external condenser of CP-1300. The objectives of PCCS are to simplify the design of nuclear power plant by the use of passive concepts and to keep the integrity and safety of the containment during the reactor accidents. PCCS is operated to remove the steam, which is generated and flows into a quiescent containment atmosphere during the postulated reactor accidents such as LOCA. The condensing tubes of PCCS ingest and cool the mixture of steam and noncondensables from the containment. The concept is similar to the PCCS of SBWR[6, 7, 8], but it is adopted to apply to CP-1300 with concrete containment. Heat transfer of condensing steam in the

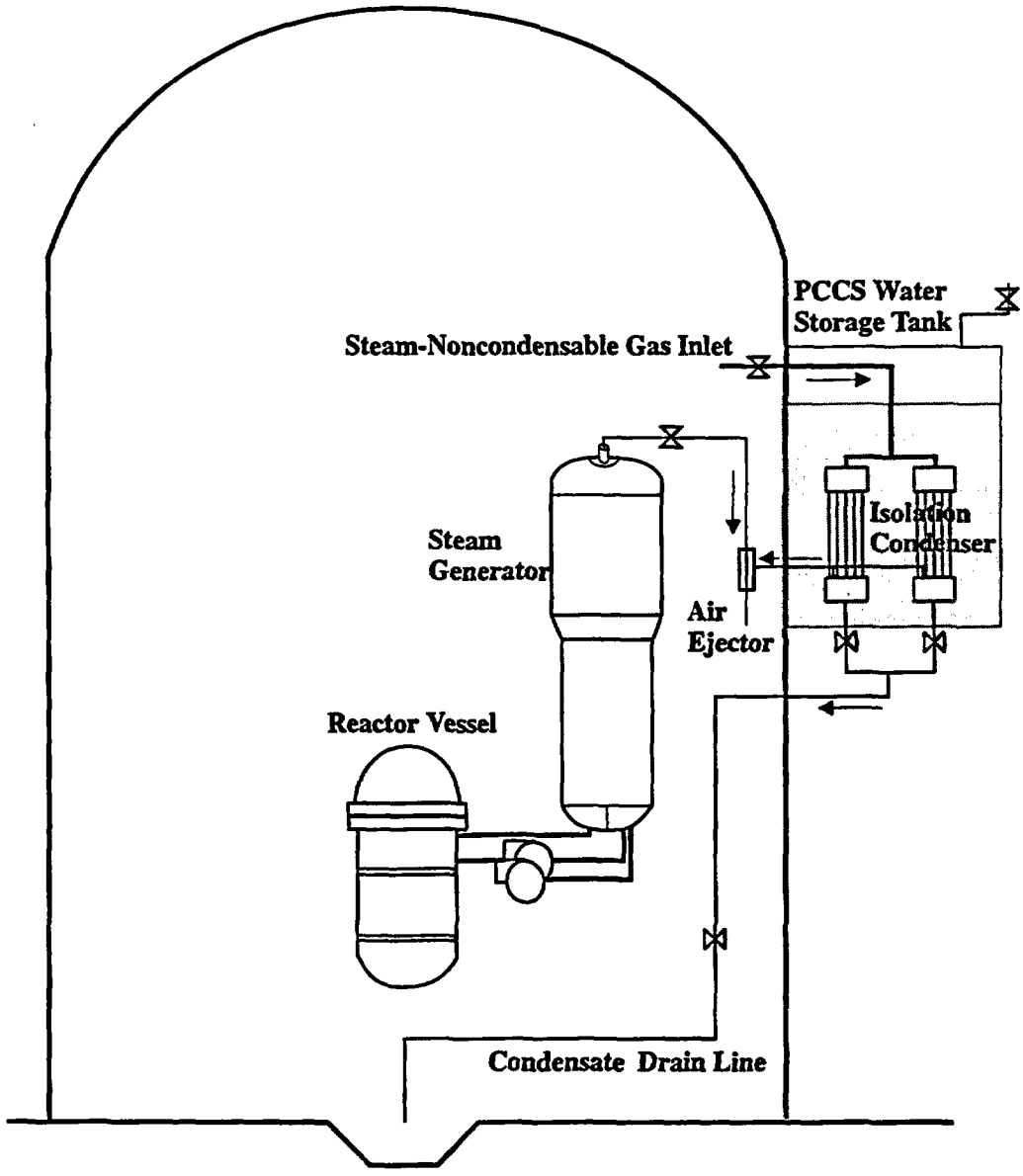

Figure 1.1: Passive containment cooling system of CP-1300

presence of noncondensables in a vertical tube of PCCS is necessary to be investigated to design the PCCS for the CP-1300 and for the SBWR as well.

The local heat transfer phenomena in a vertical tube with noncondensable gases has been studied extensively by Vierow[9, 10], Ogg[11], Siddique[12, 13], Hasanein[14], Araki[15], and Kuhn[16], and many researchers have developed their own correlations based on their own experimental data. However, it was noticed that the existing correlations were greatly scattered when compared with the applicable experimental data. New experimental apparatus is set up to minimize the entrance effect and multi-dimensional effect, more reliable data is acquired, and the effects of the various parameters on condensation with noncondensable gas are investigated. The objectives of the present experiments are described in detail in Section 2.1.

The capability to deal with steam-noncondensable gas mixtures in vertical tubes of PCCS is also an important technical problem in the design of the PCCS, and the RELAP5/MOD3.2 code is selected to simulate it.

The RELAP5/MOD3.2 code is an advanced best-estimate thermal-hydraulic transient analysis code developed at INEL under the sponsorship of the U.S.NRC. The code has been developed primarily to perform LOss of Coolant Accident(LOCA) analysis for pressurized water reactor systems. However, being a generic code, the code can be used to simulate various system configurations so that it has been extensively used for various simulation, validation, experimental data analysis and for plant/system analysis purposes. It has been exhaustively assessed with the various experimental data and extensively applied in evaluating the safety of both the commercial nuclear power plants and the next generation of advanced passive reactor designs such as SBWR, AP600, and CP-1300. It was also applied to non-LOCA, transient thermal hydraulic analysis for steam-water-noncondensable mixtures[17].

However, it is known that some heat transfer correlations in RELAP5/MOD3.2 have much uncertainties in predicting condensation-related phenomena. In particular, more reliable model is needed on condensation phenomena with noncondensable gases in a vertical tube, which is applicable to the design of the PCCS and SC of CP-1300.

1.2 Objectives and Report Organization

The main objective of the present work is to assess the capability of the RELAP5/MOD3.2 code on the condensation of the steam-noncondensable gas mixture in a vertical tube representing condensing tubes in PCCS.

For this purpose, firstly a set of experiments were performed to get a reliable data on the condensation heat transfer coefficient of the steam-noncondensable gas mixture in a vertical tube. Secondly two wall condensation models of RELAP5/MOD3.2 were assessed for steam condensation experiments in the presence of noncondensables. The condensation heat transfer database was constructed by collecting the available local data[18], and the calculation results with two wall film condensation models in RELAP5/MOD3.2 were compared with the constructed database to investigate their abilities to predict the heat transfer characteristics. Also to evaluate the code predictability, the test facility was modeled so as to be suitable for simulating the important experimental parameters in condensation experiments, and the simulation results were analyzed.

In Chapter 2 the experimental facility, its instrumentation, the test matrix, and the experimental procedure were described briefly and the experimental results were discussed in detail. In Chapter 3 the RELAP5/MOD3.2 code was described briefly, their two condensation models themselves were assessed directly with the constructed database, the nodalization of the experimental apparatus was summarized, and the simulation results from the base case calculations, the nodalization study, and the sensitivity study were analyzed and discussed. The runs statistics were also described. In Chapter 4 the conclusions and recommendations were summarized. Finally the experimental test facility and its instrumentation were described in detail in Appendix A and the data reduction method was described in Appendix B. Also the RELAP5/MOD3.2 input decks for the present experiments was listed in Appendix C.

Chapter 2

Condensation Experiments

2.1 Objectives of the Present Experiments

The steam condensation phenomena in a vertical tube with noncondensable gas has begun to be investigated just recently. Experiments have been performed by Vierow[9, 10], Ogg[11], Siddique[12, 13], Hasanein[14], Araki[15], and Kuhn[16]. However the scattering of each experimental data is large and they give different experimental results one another. It is due to the different experimental objectives and operating ranges. As an example two typical experimental works were compared, which are performed by Siddique and by Kuhn. Kuhn's experiment covered lower inlet noncondensable gas mass fractions and higher steam flow rates than Siddique's, as shown in Table 2.1.

Differences between two experiments also include steam properties, air mass fraction, Reynolds number, etc. Siddique[12] performed experiments at relatively lower steam flow rates and Kuhn[16] did at relatively higher steam flow rates. As a result, two experiments provided a quite a different results of the heat transfer coefficient.

The present experiments are performed at the steam flow rates of 8 to $40 kg/hr$. The first objective of the present experiment is to get more reliable data within all operating ranges, and the second one is to understand the effects of the various parameters on the condensation heat transfer in the presence of noncondensable gas in a vertical tube.

Table 2.1: Comparison of experimental operating ranges between Siddique's and Kuhn's

Parameters	Siddique[MIT]	Kuhn[UCB]
Inlet mass fraction(%)	10 - 35 2 - 10	0 - 40 for Air 0 - 15 for Helium
Steam flow(kg/hr)	8 - 32	30 - 60
Vapor super-heat (^oC)	none	0 - 29.3 for Air 0 - 12.5 for Helium
Mixture T.(^oC)	100, 120, 140	super-heated
Mixture pres.(kpa)	saturated	114.3 - 517.4 for Air 388.0 - 433.0 for Helium
Inlet mixture Reynolds number	5000 - 22700 5000 - 11400	13000 - 45600 for Air 13100 - 31400 for Helium
Heat transfer coefficients ($W/m^2 \cdot^o C$)	100 - 25000 high variation sensitive to Re_{mix}	500 - 8000 low variation insensitive
Steam supply	four 7kW heaters	UCB steam supply system
Coolant water T.	center of the annulus air-vortex induced turbulence	inner and outer surface $k-\epsilon$ model
Mass fraction	high variation	low variation

2.2 Test Facility and Its Instrumentation

To meet the above objectives the present experimental apparatus is newly designed to simulate the condensation phenomena of steam-noncondensable gas mixture in a vertical condensing tube.

The followings are considered to design a peculiar experimental apparatus.

1. Since the steam-air mixture velocity should be fully developed in the annulus to calculate the heat flux accurately, a honey comb is used to give the uniform initial velocity in the inlet of the coolant jacket.

2. The exit of the coolant jacket is designed to reduce the flow resistance and to minimize multi-dimensional effect.

3. Two suface temperatures in the coolant annulus are measured at every axially local positions, and the coolant bulk temperatures are calculated using an unique calculation methodology.

4. The local heat flux is directly measured with a RdF heat flux sensor at a certain location, and it is compared with the calculated heat flux from the temperature gradient of the coolant bulk temperatures.

The schematic diagram of the experimental facility is shown in Figure 2.1. The experimental facility consists of a steam tank including a $100kW$ heater, a steam-noncondensable gas mixture supply line, a test section with a condensing tube and its surrounding coolant jacket, a lower plenum, venting and draining systems, and a unit of data acquisition system. The steam tank functions as a containment. Steam is generated from the steam tank and is mixed with the supplied noncondensable gas in the steam tank. The noncondensable gas is supplied into the steam tank continuously to give a continuous noncondensable gas mass fraction at the inlet of the test section, or to keep a total air inventory in the tank by the noncondensable gas supply line. The steam-noncondensable gas mixture flow is made to keep uniform velocity distribution, and its temperature and pressure are measured in the inlet of the test section.

The test section consists of an inner condensing tube and an outer coolant jacket. The inner tube of the heat exchanger is a stainless steel pipe of $50.8mm$ in outer diameter, $1.5mm$ in thickness, and $2400mm$ in length. At 12 different axial locations each J-type thermocouple is welded on the outer surface of the condensing tube to measure the outer surface temperatures, welded through the condensing tube to measure the mixture bulk temperatures, and installed on the outer wall of the coolant annulus to measure the adiabatic wall temperatures. These three kinds of temperature sensor are located irregularly so that the total heat transfer is kept to be same in the interval between two close temperature measuring probes. The cooling water flows upward through the annulus and the steam-noncondensable gas mixture flows downward in a condensing tube. The cooling water is supplied to the lower

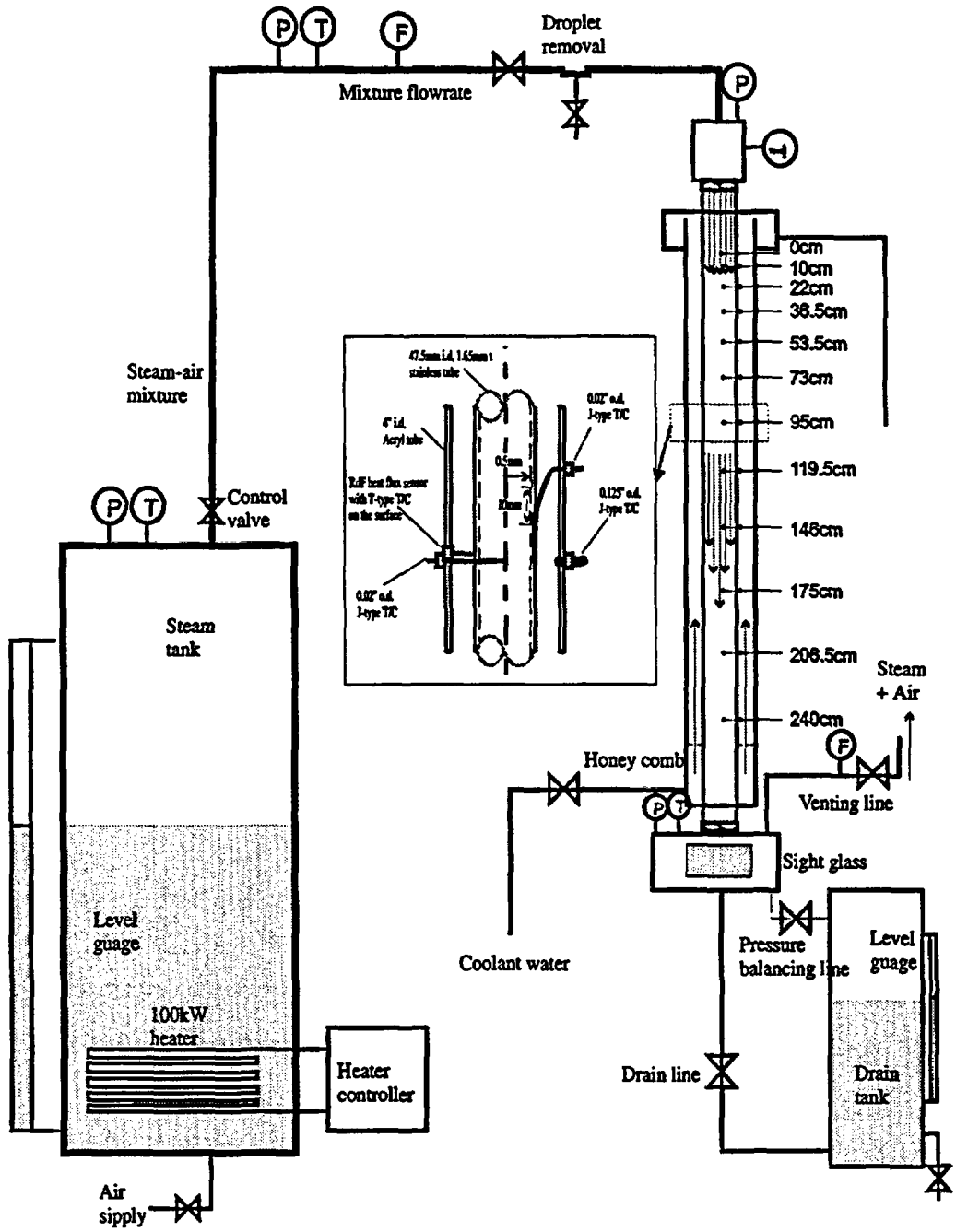

Figure 2.1: A schematic diagram of KAIST condensation experimental apparatus

end of the jacket pipe in an once-through mode by a calibrated rotameter and a flow control valve, and is dumped to the drain after the increase of its temperature.

Table 2.2 summarizes the instrumentation of KAIST condensation experimental apparatus and their uncertainties.

Table 2.2: Instrumentation of KAIST condensation experimental apparatus

Parts	Measuring parameters	Model number	Measuring ranges	Units	Uncertainty
Steam tank	Pressure	ABB PT-624	0 - 8.0	kg_f/cm^2	0.1%
	Temperature	OMEGA KMQSS	max. 1000	^oC	0.5%
Air source	Flow rate	Dwyer RMC-103	20 - 200	SCFH	2%
	Pressure	OMEGA PX-425	0 - 100	psig	0.2%
T/S : inlet	Pressure	OMEGA PX-425	0 - 100	psig	0.2%
	Temperature	OMEGA JMQSS	max. 500	^oC	0.5%
	Flow rate	OMEGA FV-510B	0 - 500	lb/hr	1.5%
T/S : tube	Mixture bulk T.	OMEGA JMQSS	max. 500	^oC	0.5%
	Outer wall T.	OMEGA JMQSS	max. 500	^oC	0.5%
	Heat flux	RdF 20453-1	0 - 50	Btu/ft^2s	5%
T/S : coolant	Temperature	OMEGA JMQSS	max. 500	^oC	0.5%
	Flow rate	Dwyer RMC-142	0.2 - 2.2	gpm	2%
Lower plenum	Pressure	OMEGA PX-425	0 - 100	psig	0.2%
	Temperature	OMEGA JMQSS	max. 500	^oC	0.5%
Drain plenum	Pressure	Foxboro E11AH	0 - 750	kpa	0.5%
	Temperature	OMEGA JMQSS	max. 500	^oC	0.5%
Venting plenum	Pressure	OMEGA PX-425	0 - 100	psig	0.2%
	Temperature	OMEGA JMQSS	max. 500	^oC	0.5%
	Flow rate	Dwyer VFB-53	10 - 100	SCFH	3%

All the signals from detectors are current outputs or voltage outputs including outputs from thermocouples. $4 \sim 20mA$ current signals from the pressure transducer and the vortex flow meter are converted to $1 \sim 5V$ voltage signals using an multi-channel current-to-voltage converter. The temperature signals are compensated to give accurate temperature data. All signals are applied to the Hewlett Packard 44708H high voltage relay multiplexer to give a reliable temperature and voltage data. Sampled experimental data is acquired using the

HP3852A control unit and the data is transferred to IBM-PC/AT using the RS232C interface.

The test facility and its instrumentation are described in detail in Appendix A.

2.3 Test Matrix and Experimental Procedure

As shown in Table 2.3, total 19 sub-tests were performed varying the following input parameters: the saturated steam temperature at the inlet, T_{in}, the inlet air mass fraction, AMF, its inlet total pressure, P_{tot}, the inlet steam flow rate, SF, and the inlet air flow rate, AF. These

Table 2.3: Test matrix of KAIST condensation experiment

I.D.	T_{in} (^oC)	AMF	P_{tot} (kpa)	SF (kg/h)	AF (kg/h)	Exp. No.
T1A2a	110.4	0.204	168.4	22.0	5.5	E13c
T1A3a	110.7	0.297	185.4	7.6	3.2	E9b
T1A3b	110.5	0.303	185.4	18.2	7.8	E13b
T1A4a	110.8	0.395	207.3	7.7	4.9	E9a
T1A4b	110.5	0.407	208.2	11.7	7.9	E13a
T2A1a	120.5	0.103	216.6	25.7	2.9	E11f
T2A2a	121.4	0.195	239.0	14.8	3.6	E4a
T2A2b	121.4	0.200	239.9	21.3	5.2	E11d
T2A2c	120.8	0.196	234.4	25.8	6.2	E11e
T2A3a	120.9	0.306	260.8	9.8	4.3	E11b
T2A3b	120.4	0.297	254.9	15.2	6.4	E7a
T2A3c	120.5	0.296	254.5	16.5	6.8	E11c
T2A4a	120.9	0.408	292.0	9.5	6.4	E11a
T3A1a	129.0	0.102	281.3	32.8	3.7	E4d
T4A1a	137.7	0.105	363.6	40.0	4.6	E8e
T4A2a	143.4	0.215	465.5	32.7	8.8	E12b
T4A3a	140.4	0.301	463.2	18.4	7.8	E12a
T4A3b	139.6	0.307	456.2	19.9	8.7	E8b
T4A4a	140.6	0.363	498.4	18.8	10.5	E8a

experiments span the ranges of conditions expected for the PCCS design. These sub-tests can be grouped into four cases by inlet saturated steam temperatures: T1 series(110^oC); T2 series(120^oC); T3 series(130^oC); and T4 series(140^oC). In each group, the effect of inlet air

mass fraction and inlet steam-air mixture flow rate were investigated.

The steam-noncondensable gas mixture in the test section is in a saturated state, and the system pressure is the sum of the saturated steam pressure and the partial pressure of the noncondensable gas.

The test procedures are as follows:

1. At the beginning, the steam tank is isolated from the rest of the system.
2. The water level of the steam tank is adjusted and recorded.
3. The noncondensable gas is removed from, or supplied to the steam tank to meet a predetermined initial condition.
4. The heater is turned on and the water is boiled to reach the required initial temperature and pressure from which the initial air mass fraction can be calculated.
5. The heater is controlled to generate the steam to give a predetermined pressure.
6. The coolant flow rate is adjusted to the determined value.
7. The air is injected into the tank to keep a constant initial condition.
8. After the heater power is readjusted, the accumulated air is vented and the condensate is drained to stabilize the system pressure.
9. Data are acquired from sensors and transducers after the steady state is achieved.
10. The local heat transfer coefficients and the other reduced data are calculated from the raw data.

2.4 Experimental Results and Discussions

As steam-noncondensable gas mixture enters into a vertical condensing tube of the PCCS, as shown in figure 2.2, steam begins to condense at the inlet of the tube. The steam condenses on

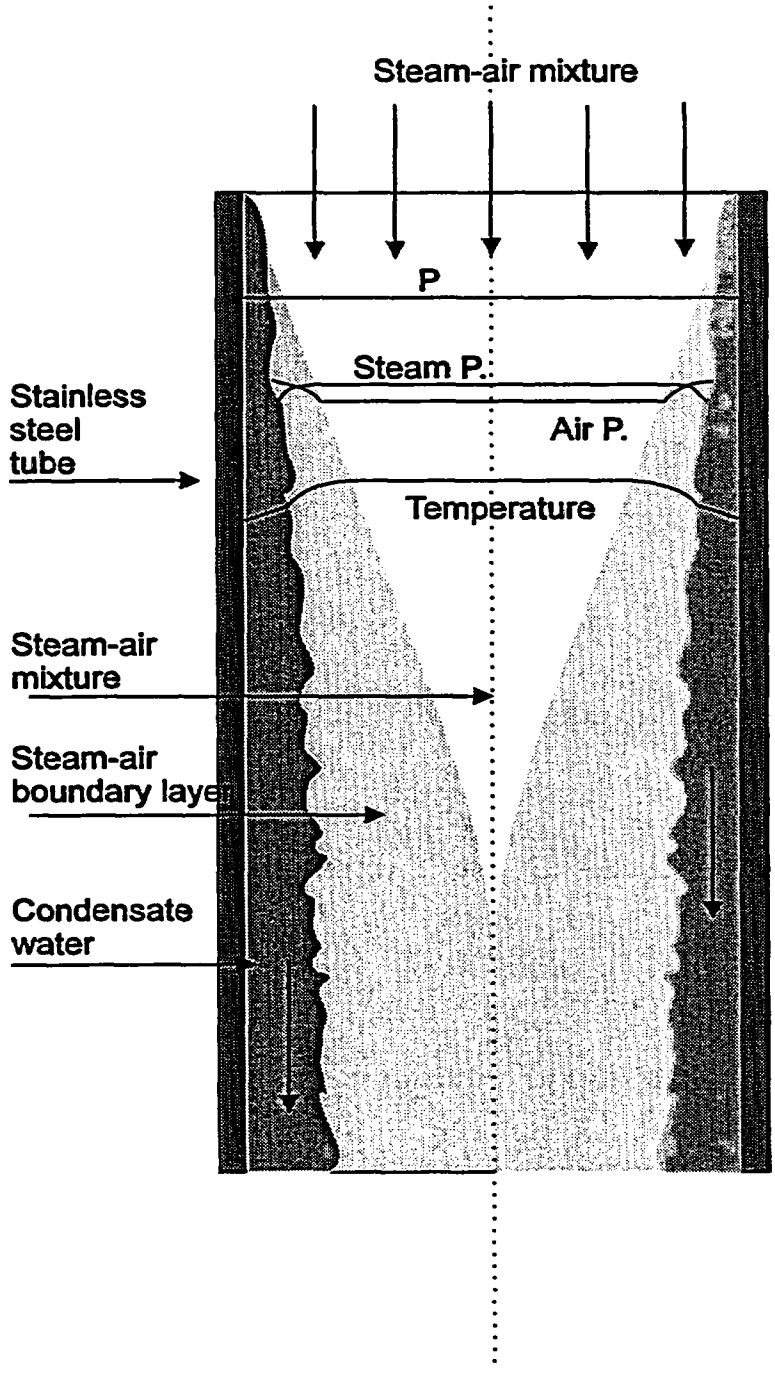

Figure 2.2: Condensation phenomena in a vertical tube in the presence of noncondensable gas

the inner wall of the tube and the condensed film flows as an annular film along the condensing tube. A gas-vapor boundary layer forms next to the condensate interface, through which the water vapor must pass by diffusion and convection, and it thickens between the condensate film layer and the steam-noncondensable gas mixture layer. The partial pressures of gas and vapor vary through the boundary layer. At a certain axial location, the boundary layer grows and blocks the tube and there is no longer a central core.

Generally both the local air mass fraction and the local condensate flow rate increases, but the local steam-air mixture flow rate decreases along the condensing tube.

Temperatures of the coolant, the outer wall of the tube, and the steam-air mixture bulk are measured. The coolant bulk temperature is calculated by the unique numerical calculation method using two suface temperatures and the coolant flow rate in the coolant annulus. The local heat flux is calculated from the profile of the coolant bulk temperature, and the inner wall temperature of the test section is calculated from the outer wall temperature of the condensing tube and the calculated heat flux. The local heat flux at $1.75m$ apart from the tube inlet is directly measured with the RdF heat flux sensor to cross-check the calculated heat flux.

The data reduction method is described in detail in Appendix B.

Figure 2.3 shows the local temperature distributions of the steam-air mixture bulk, the inner surface, the outer surface, the coolant adiabatic, and the coolant bulk along the test section in experiment *E13b* with the inlet saturated steam temperature of 140^oC and the inlet air mass fraction of 20%. All temperatures decrease smoothly along the test section, except for the inversion of two wall temperatures.

The inversion of the outer wall temperature occurs in the middle of the condensing tube. One anticipated reason for such a temperature inversion is from the mechanical error by wrong silver soldering, and another reason is the secondary flow of the coolant flow in an annulus jacket, which is originated from Hasanein[14]. To determine whether the temperature inversion is caused by the secondary flow or not, the radial temperature distribution is planned to check. The coolant temperatures are measured with movable thermocouples for several

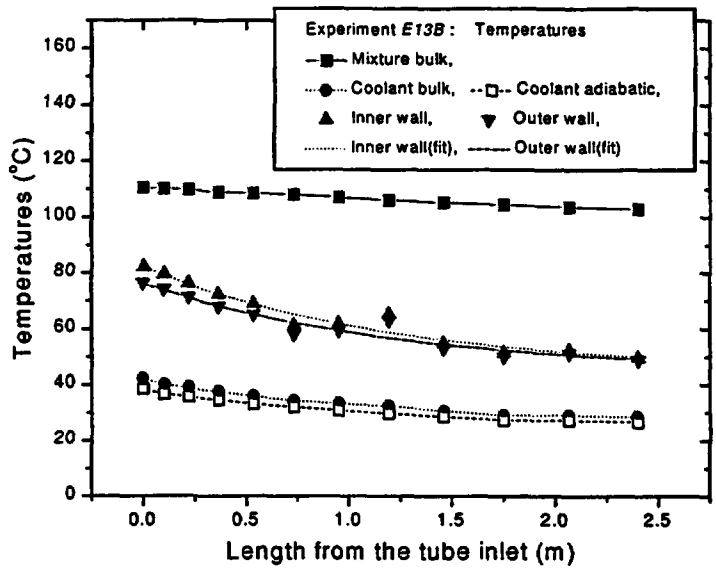

Figure 2.3: Local temperature distributions in experiment *E13b*

radial points at 5 axial locations, which are near the position of the temperature inversion. The measured outer wall temperatures are fitted to give a smooth slope along the test section, and the inner wall temperatures are calculated again.

As shown in Figure 2.4, generally the local heat flux decreases rapidly as the local air mass fraction increases and the local mixture flow rate decreases along the condensing tube. The local heat flux at $1.75m$ apart from the tube inlet is directly measured with the RdF heat flux sensor, and it gives the heat flux similar to the calculated one.

Some sub-tests are compared to investigate the parametric effects of the condensation experiments.

2.4.1 Effects of inlet steam-air mixture flow rate

The comparisons are performed at three different inlet steam flow rates of 15, 21, and $26kg/hr$ for a condition of air mass fraction of 20% and a saturated steam temperature of $120°C$. Figure 2.5 and 2.6 show comparisons of both experimental heat fluxes and heat transfer coefficients with different inlet steam-air mixture flow rate, respectively.

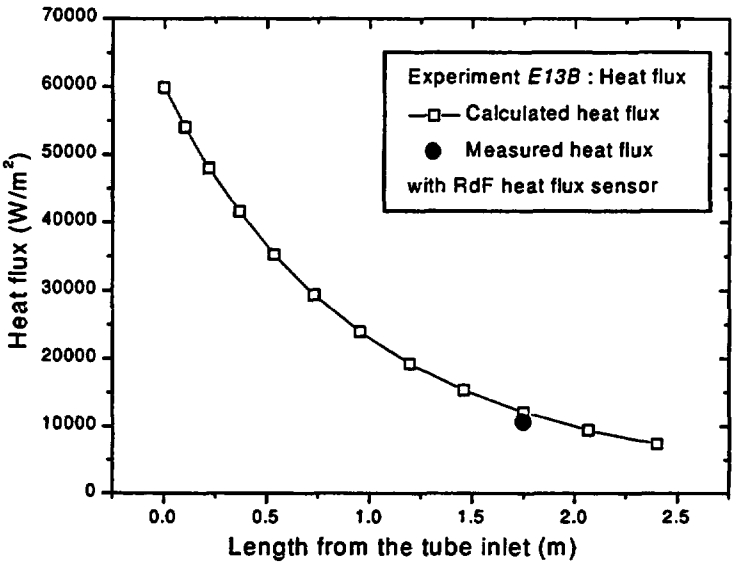

Figure 2.4: Local heat flux distribution in experiment *E13b*

As shown in Figure 2.5, with higher inlet steam-air mixture flow rate, the local heat flux decreases more smoothly in the inlet, and it always keeps higher values throughout the condensing tube than that with lower one. It is due to the fact that it keeps an higher local mixture Reynolds number along the condensing tube with a high inlet mixture flow rate.

In the inlet of the test section, it gives similar value regardless of the different initial mixture flow rate. As the condensate liquid film just begins to develop and the mixture boundary layer is not developed, the mixture is almost directly in contact with the outer wall of the condensing tube in that region. It is considered that heat flux depends only on the air mass fraction and the saturated steam temperature in that region.

Since more steam is removed from the steam-air mixture flow with higher inlet mixture flow throughout the condensing tube, the local steam flow rate is decreased, and the local air mass fraction is increased rapidly along the condensing tube. Thus the heat flux becomes similar also in the outlet of the test section.

As shown in Figure 2.6, the heat transfer coefficient shows the similar tendencies to the heat flux. It is shown to be similar regardless of the inlet mixture flow rate both in the inlet

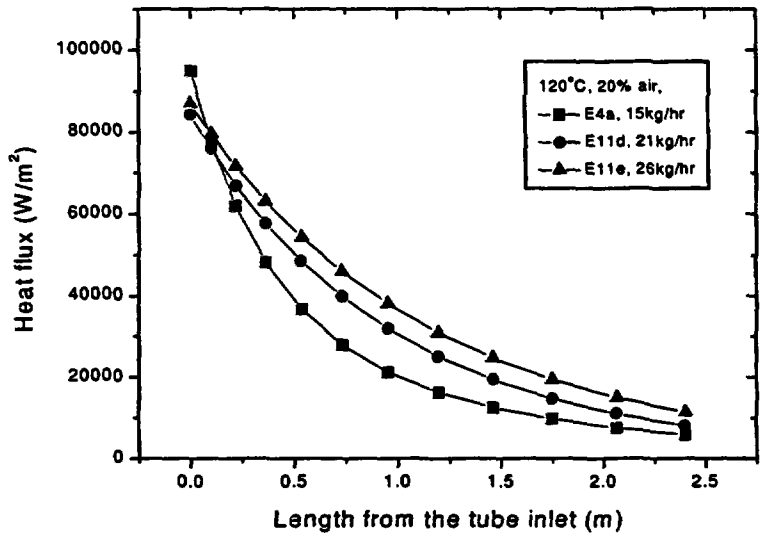

Figure 2.5: Comparison of experimental heat fluxes with the variation of the inlet steam-air mixture flow rate

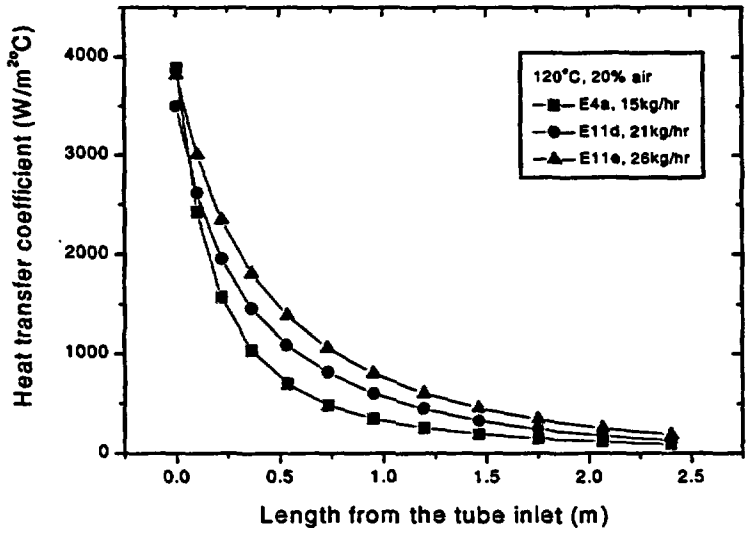

Figure 2.6: Comparison of experimental heat transfer coefficients with the variation of the inlet steam-air mixture flow rate

and in the outlet of the condensing tube, but it always keeps higher values with higher inlet mixture flow rate throughout the condensing tube.

Figure 2.7 shows the axial temperature distributions of the steam-air mixture bulk, the inner surface, the outer surface, the coolant adiabatic, and the coolant bulk along the test section for experiments *E4a*, *E11d*, and *E11e* with different initial steam-air mixture flow rate. All the five temperatures show smoother profiles with a higher steam-air mixture flow rate than with a lower one.

The air contained inside the test section must be vented to initiate the condensation of the steam in the presence of air, to maintain a constant pressure, and to prevent the accumulation of the air throughout the test section. As the steam-air mixture penetrates more deeply, higher mixture bulk temperature is kept throughout the test section, which is the main cause of the smoother temperature distribution and the higher heat transfer.

2.4.2 Effects of inlet air mass fraction

The comparisons are performed at 2 different values of the inlet air mass fractions of 20, and 30% for a fixed inlet saturated steam temperature of $110^{o}C$ and inlet mixture flow rate of about $20kg/hr$. Figure 2.8 and 2.9 show comparisons of both experimental heat fluxes and heat transfer coefficients with different inlet air mass fraction, respectively.

As shown in Figure 2.8, the local heat flux is much higher in the inlet of the test section with lower inlet air mass fraction. It decreases more rapidly throughout the condensing tube than that with higher inlet air mass fraction, and as a result it becomes similar in the outlet of the condensing tube. The local air mass fraction is always kept low with low inlet air mass fraction along the condensing tube. With lower air mass fraction, more steam is removed from the steam-air mixture flow throughout the condensing tube. As the local mixture flow rate is decreased and the local air mass fraction is increased, the heat transfer by condensation is reduced and the heat transfer by convection of mixture becomes dominant in the outlet of the test section.

As shown in Figure 2.9, the heat transfer coefficient shows the similar tendencies to the

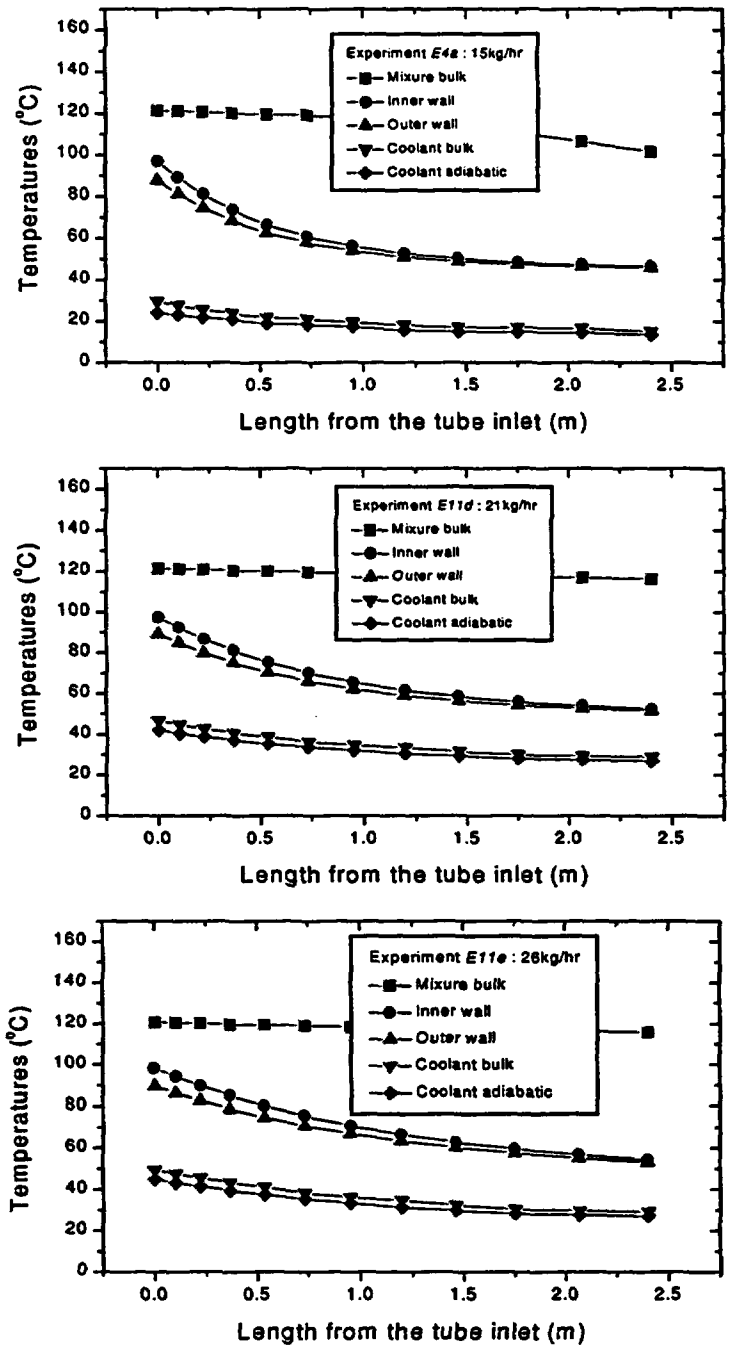

Figure 2.7: Comparison of experimental temperature distributions with the variation of the inlet steam-air mixture flow rate at the inlet mixture temperature of $120°C$ with 20% air

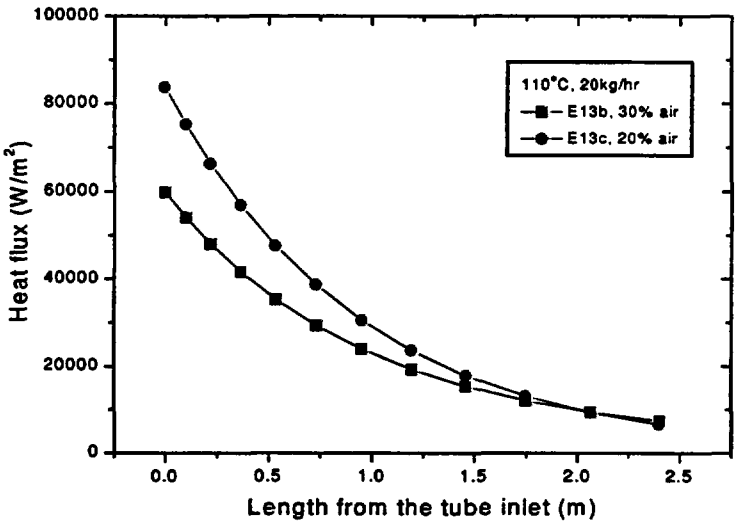

Figure 2.8: Comparison of experimental heat fluxes with the variation of the inlet air mass fraction

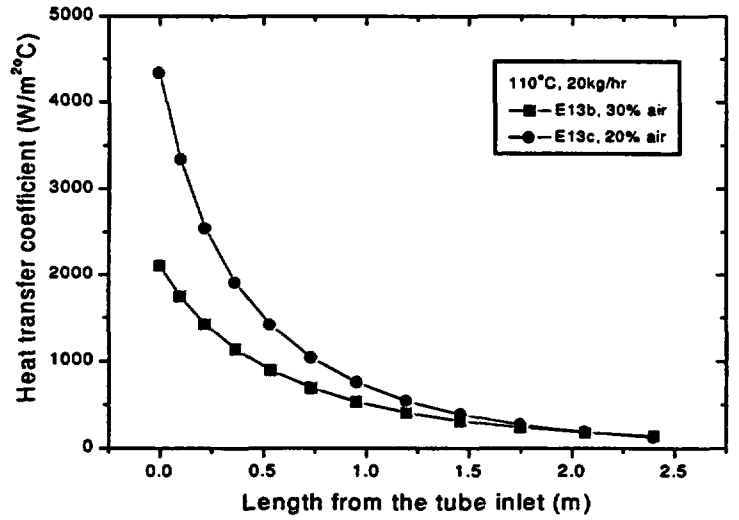

Figure 2.9: Comparison of experimental heat transfer coefficients with the variation of the inlet air mass fraction

heat flux. It is shown to be much higher in the inlet, and always keep higher value throughout the condensing tube with higher inlet air mass fraction, and it becomes similar in the outlet of the condensing tube regardless of the inlet air mass fraction.

2.4.3 Effects of inlet saturated steam temperature

The comparisons are performed at 2 different values of the inlet saturated steam temperatures of 110 and 140^oC for a fixed air mass fraction of 30% and a steam flow rate of about $18kg/hr$. Figure 2.10 and 2.11 show comparisons of both experimental heat fluxes and heat transfer coefficients with different inlet saturated steam temperature, respectively.

As shown in Figure 2.10, the local heat flux is always much higher with the increase of the inlet saturated steam temperature in the inlet of the test section, but the difference between heat fluxes of different inlet saturated steam temperature is negligible in the outlet of the test section.

However, as shown in Figure 2.11, the local heat transfer coefficient decreases more rapidly with higher inlet saturated steam temperature. It always keeps lower value throughout the condensing tube than that with low saturated steam temperature, except for the inlet of the test section, where it gives similar values regardless of the different inlet saturated steam temperature. The higher wall sub-cooling permits higher heat flux due to the higher thermal driving force, or the temperature difference between the mixture bulk and the inner wall. However, when the heat flux is divided by the temperature difference to give the heat transfer coefficient, the local heat transfer coefficient is always lower with high inlet saturated steam temperature than that with lower one.

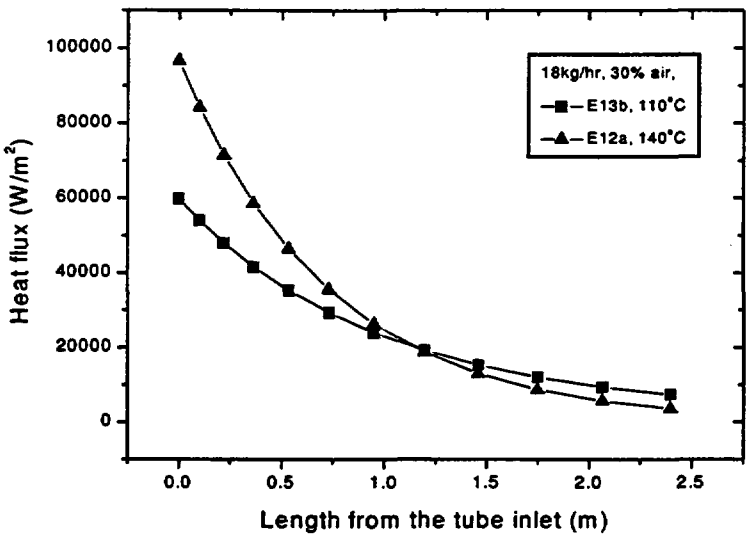

Figure 2.10: Comparison of experimental heat fluxes with the variation of the inlet saturated steam temperature

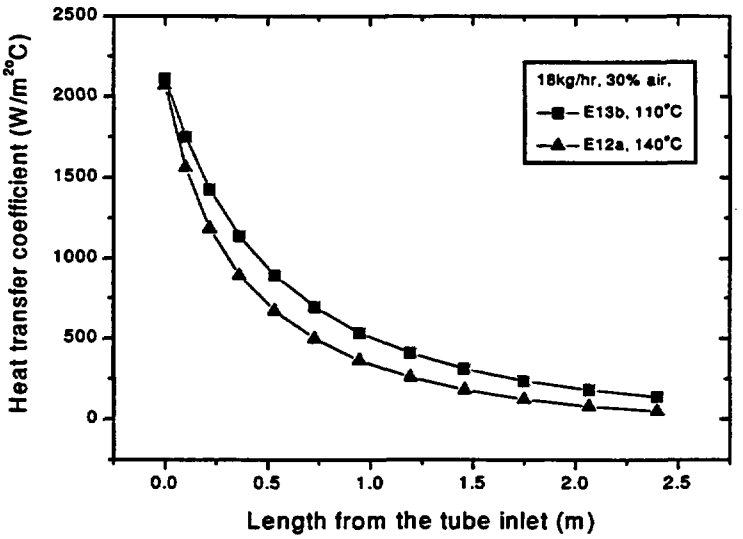

Figure 2.11: Comparison of experimental heat transfer coefficients with the variation of the inlet saturated steam temperature

Chapter 3

Assessment of RELAP5/MOD3.2

3.1 Two Wall Film Condensation Models of RELAP5/MOD3.2

A standard RELAP5/MOD3.2 was used for the present calculation. Related with the calculation for the condensation experiment with noncondensable gas in a vertical condensing tube, the RELAP5/MOD3.2 code was known to have more improved models than the previous version, RELAP5/MOD3.1, in wall condensation model and transport of non-condensable gas[19].

The condensation of steam-noncondensable gas mixture in a vertical condensing tube can be simulated with two wall film condensation models in RELAP5/MOD3.2[18]. For an inclined surface the Nusselt-Shah-Colburn-Hougen correlations are used as a default model, and the Nusselt correlation with UCB multipliers is used as an alternative model. For the horizontal case the Nusselt correlation is replaced by the Chato correlation both in the default and alternative models.

3.1.1 Default condensation model

The default model is to use the maximum of Nusselt[20]'s and Shah[21]'s with the Colburn-Hougen[22]'s diffusion calculation when noncondensable gases are present. The Nusselt[20]'s

expression for the vertical surface uses the film thickness.

$$h_f = \frac{k_f}{\delta}, \tag{3.1}$$

where the film thickness, δ, is

$$\delta = \left[\frac{3\mu_f \Gamma}{g\rho_f \Delta\rho}\right]^{1/3} = \left[\frac{3\mu_f^2 Re_f}{4g\rho_f \Delta\rho}\right]^{1/3}, \tag{3.2}$$

where Γ is the mass flux per unit width and Re_f the liquid film Reynolds number.

Chato[23] developed a modification to the Nusselt formulation which applies to the laminar condensation on the inside of a horizontal tube. The correlation takes the form

$$h_c = F\left[\frac{g\rho_f \Delta\rho h_{fgb} k_f^3}{D_h \mu_f (T_{sppb} - T_w)}\right]^{1/4}, \tag{3.3}$$

where k_f is the liquid conductivity, μ_f the liquid viscosity, ρ_f the liquid density, $\Delta\rho$ the difference in densities between the liquid and the vapor, g the gravitational constant, h_{fgb} the steam saturation enthalpy at steam partial pressure minus liquid saturation enthalpy in the bulk, and T_{sppb} the saturation temperature based on steam partial pressure in the bulk. The F is the term which corrects for the liquid level in the tube bottom and a value of 0.296 is recommended for free flow from a horizontal tube.

The Shah[21]'s model is used for the modeling of film condensation with turbulent flow as follows;

$$h_c = h_{sf}(1 + \frac{3.8}{Z^{0.95}}), \tag{3.4}$$

where

$$Z = \left(\frac{1}{X} - 1\right)^{0.8} P_{red}^{0.8}, \tag{3.5}$$

and X is the static vapor quality, P_{red} the reduced bulk pressure, $P/P_{critical}$, and h_{sf} the

superficial heat transfer coefficient, which is given by

$$h_{sf} = h_l(1 - X)^{0.8}, \tag{3.6}$$

where h_l is the Dittus-Boelter coefficient assuming all fluid is liquid, given by

$$h_l = 0.023(\frac{k_l}{D_h})Re_l^{0.8}Pr_l^{0.4}, \tag{3.7}$$

where the Reynolds number is given by $Re_l = G_{total}D_h/\mu_f$, G_{total} the total mass flux, D_h the hydraulic diameter, μ_f the liquid viscosity, and Pr_l the liquid Prandtl number. The Shah correlation is based on the database of both horizontal and vertical data, and it is activated when its heat transfer coefficient becomes larger than that of Nusselt correlation or that of Chato correlation.

The formulation of the Colburn-Hougen model is based on the principle that the amount of heat transferred by condensing vapor to the liquid-vapor interface by diffusing through the steam-noncondensable gas mixture boundary layer is equal to the heat transferred through the condensate. The heat flux due to vapor mass flux is

$$q_v'' = h_m h_{fgb}\rho_{vb} ln\left[\frac{1 - P_{vi}/P}{1 - P_{vb}/P}\right], \tag{3.8}$$

where P is the total pressure, P_{vb} the steam partial pressure in the bulk, P_{vi} the partial pressure of steam at liquid-gas-vapor interface, ρ_{vb} the saturation vapor density at P_{vb} and h_m the mass transfer coefficient. The mass transfer coefficient, h_m, depends on the flow condition. When the vapor flow is turbulent, the Gilliand correlation[24] is used, and when laminar, the Rohsenow-Choi correlation[24] is used. The heat heat flux from the liquid to the wall is calculated by

$$q_l'' = h_c(T_{vi} - T_w), \tag{3.9}$$

where T_{vi} is the saturation temperature corresponding to the interface vapor pressure, T_w the wall temperature, and h_c the predicted condensation heat transfer coefficient. From the

energy balance the partial vapor pressure at the interface and its corresponding temperature are determined by iteration.

$$h_c(T_{vi} - T_w) = h_m h_{fgb} \rho_{vb} ln\left[\frac{1 - P_{vi}/P}{1 - P_{vb}/P}\right]. \tag{3.10}$$

3.1.2 Alternative condensation model

The alternative model is the Nusselt model with UCB multipliers, which is revised to include the effects of the interfacial shear and the presence of the noncondensable gas in a vertical tube as follows:

$$h_{UCB} \cdot \frac{\delta}{k_f} = f_1 \cdot f_2, \tag{3.11}$$

where f_1 and f_2 are formulated from the curve fits to the experimental data as follows:

$$f_1 = 1 + 2.88 \times 10^{-5} Re_{mix}^{1.18}, \tag{3.12}$$

where the steam-noncondensable gas mixture Reynolds number is given by $Re_{mix} = G_g D_h / \mu_g$, where G_g is the gas bulk mass flux, D_h the hydraulic diameter, and μ_g the gas bulk viscosity.

$$f_2 = \begin{cases} 1 - 10 M_a & for \quad M_a < 0.063, \\ 1 - 0.938 M_a^{0.13} & for \quad 0.063 < M_a < 0.6, \\ 1 - M_a^{0.22} & for \quad M_a > 0.6, \end{cases} \tag{3.13}$$

where M_a is the fraction of noncondensable gas in the vapor-gas mixture. In this alternative model the Nusselt correlation and the UCB f_1 factor is used instead of the maximum of the Shah and the Nusselt correlation in the default model, and the UCB f_2 factor instead of the Colburn-Hougen diffusion method. The enhancement factor, f_1, accounts for the effects of the shear of the steam-noncondensable gas mixture on the liquid film, and the degradation factor, f_2, accounts for the effects of the noncondensable gas on the heat transfer coefficient. The maximum value allowed for f_1 is 2.0 to prevent over-predicting in the high shear region such as in the entrance region. For a horizontal tube with laminar flow the Nusselt correlation

is also replaced by the Chato correlation.

3.2 Direct Assessment of Two Wall Film Condensation Models

The condensation models in RELAP5/MOD3.2 require various local properties to give condensation heat transfer rates. The condensation heat transfer database is constructed by collecting the local data in literature or by calculating the local parameters from the correlations published[18]. It is done on the basis of local values to ease handling of the database and assessment with correlations. The detailed information of the constructed database is given in Table 3.1.

Table 3.1: Heat transfer database for the vertical laminar film condensation

Author	Data #	Run	Pressure (MPa)	Steam flow (kg/h)	NC gas	
					Non	air fraction
Vierow[9]	297	36	0.03 ~ 0.45	5.9 ~24.95	air	0 ~ 0.14
Siddique[12]	319	42	0.109 ~ 0.518	28.3 ~ 61.5	none	0
	416	52	0.107 ~ 0.485	7.9 ~ 31.9	air	0.08~ 0.42
	159	22	0.114 ~ 0.466	8.6 ~ 20.5	He	0.02~ 0.11
Hasanein[14]	291	44	0.101, 0.27	10 ~ 40	He	0.025 ~ 0.2
	600	76	0.101, 0.27	10 ~ 40	air	0.05~ 0.2
					(He)	(0.025)~ (0.15)
Kuhn[16]	627	71	0.114 ~ 0.517	29.5 ~ 61.0	air	0.01~ 0.4
	192	24	0.388 ~ 0.433	29.5 ~ 61.9	He	0.003~ 0.15

Since the constructed database can give all local values which are required by the two wall film condensation models in RELAP5/MOD3.2 code, those models can be assessed directly, or the heat transfer coefficients calculated directly with two condensation models themselves are compared with those from the constructed data base. Therefore, it does not cause any systematic effect which might occur from the internal code calculation. Both the default and the alternative models used for the laminar film condensation heat transfer inside a vertical

condensing tube are assessed.

In the case of the default model, its prediction is compared with the Hasanein[14]'s experimental data to assess the Colburn-Hougen diffusion method[22].

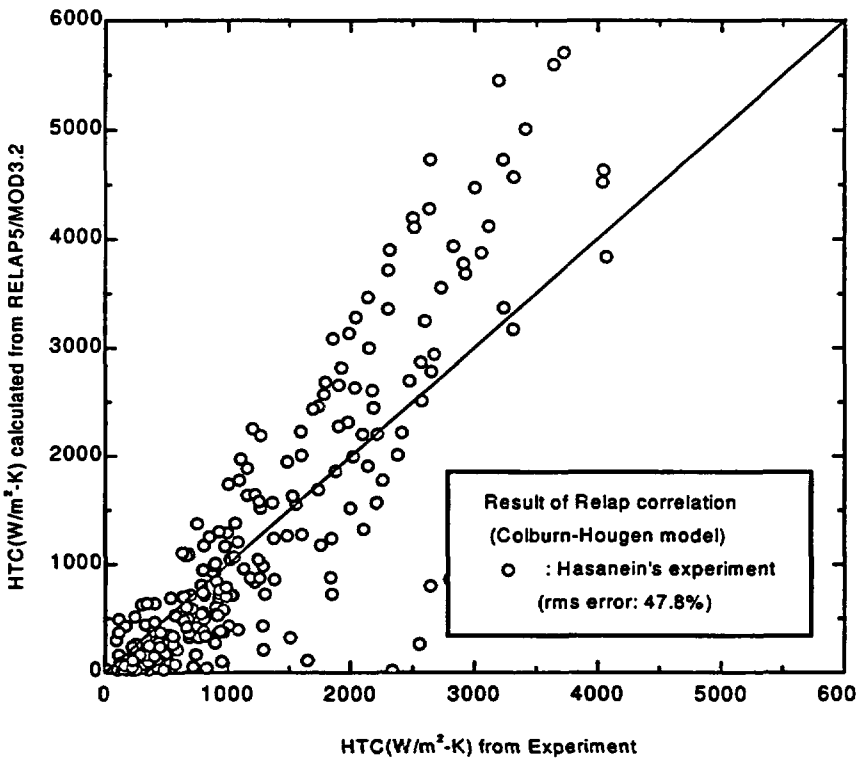

Figure 3.1: Assessment of default model of RELAP5/MOD3.2

For the Hasanein's data[14] the RELAP5/MOD3.2 model under-predicts the experimental data for the low heat transfer coefficient range, but it over-predicts the experimental data for the high heat transfer coefficient range as shown in Figure 3.1. As the heat transfer coefficients calculated from the default model show much large scattering, a modification of the Colburn-Hougen diffusion method is needed for a better prediction of laminar film condensation with noncondensable gas.

In the case of the alternative model, its predictions are compared with 3 kind of experiments for pure steam, steam-air, and steam-helium condensation. Figure 3.2 shows the

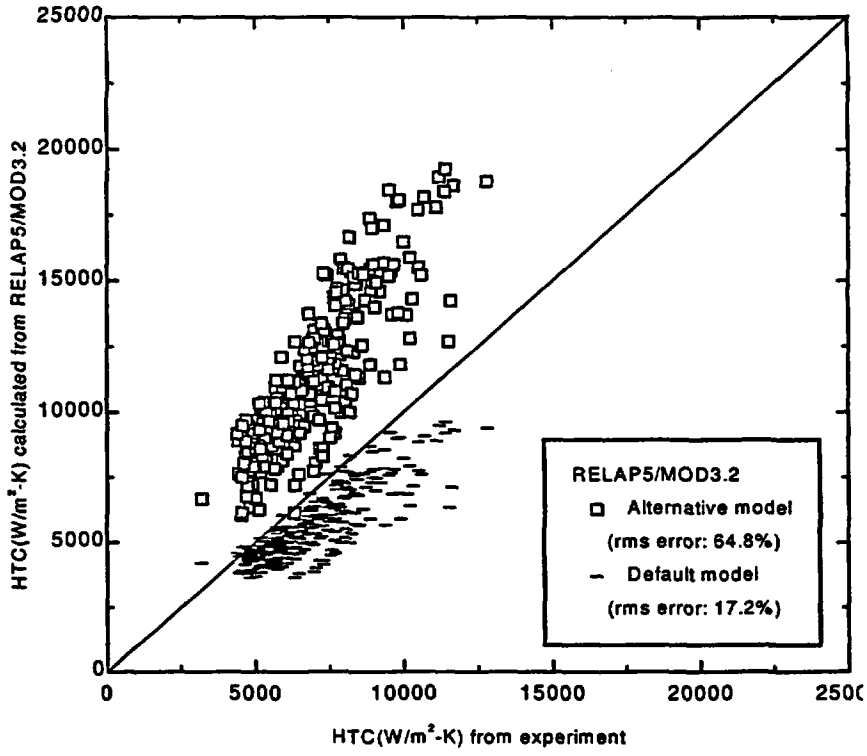

Figure 3.2: Assessment of two wall film condensation models of RELAP5/MOD3.2 for pure steam

assessment results for the alternative model of RELAP5/MOD3.2 with Kuhn's[16] experimental data for pure steam. Since the effect of the shear stress of steam flow was included in Kuhn's data to increase the heat transfer coefficient, the prediction of the Nusselt correlation shows a little smaller than Kuhn's experimental data. The predicted value of the alternative model of RELAP5/MOD3.2 is always higher than that of the Nusselt correlation by almost 2 times, and it gives higher values compared with the Kuhn's experimental data. The effect of shear stress by the steam flow is overestimated. For most of the experimental data compared, the enhancement factors, f_1, have the limit values of 2. As Kuhn's experiments are performed at high mixture Reynolds numbers, its data exceed the operating range of UCB correlation in the alternative model of RELAP5/MOD3.2.

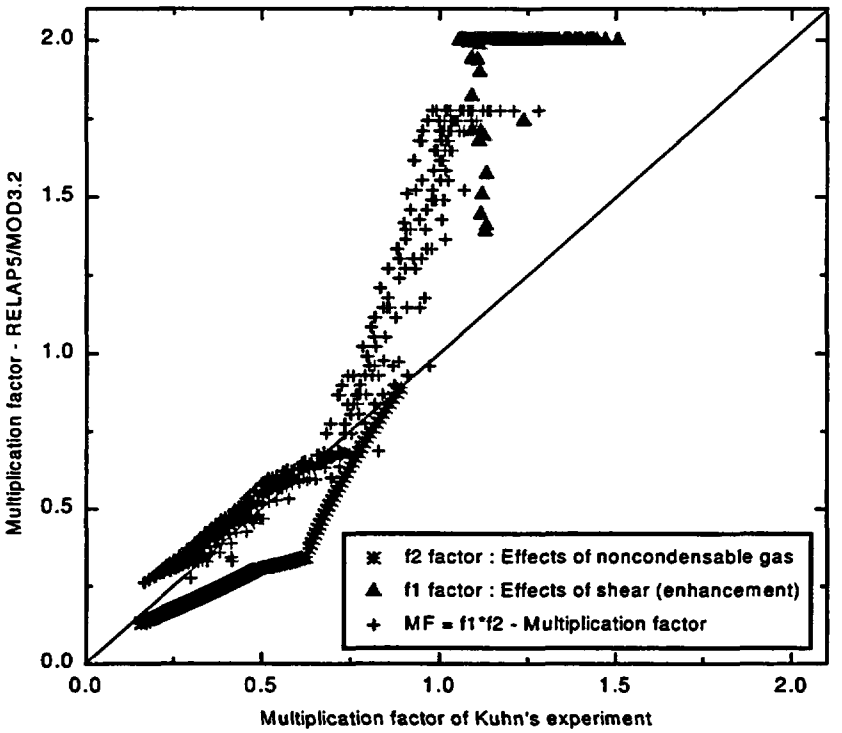

Figure 3.3: Multiplication factors in alternative model of RELAP5/MOD3.2

Comparison of multiplication factors in the alternative model of RELAP5/MOD3.2 with the Kuhn's air-steam experimental data is shown in Figure 3.3. The enhancement factor, f_1, the degradation factor, f_2, and the overall multiplication factor, f, are compared. Similar to the assessment results for the pure steam condensation, the f_1 factor converges to the limit value of 2 for the experiment with noncondensable gases. The degradation factor f_2 is also calculated using equation 3.13 with Kuhn[16]'s raw data. f_1 and f_2 is multiplied to give the overall multiplication factor, f. For the low heat transfer coefficient range with high air mass fraction and low shear stress the overall multiplication factors of both Kuhn's[16] and RELAP5/MOD3.2 correlation give similar results as the overestimation of f_1 is compensated by the underestimation f_2. However, the multiplication factor f is overestimated by the alternative model for a range to produce the high heat transfer coefficients.

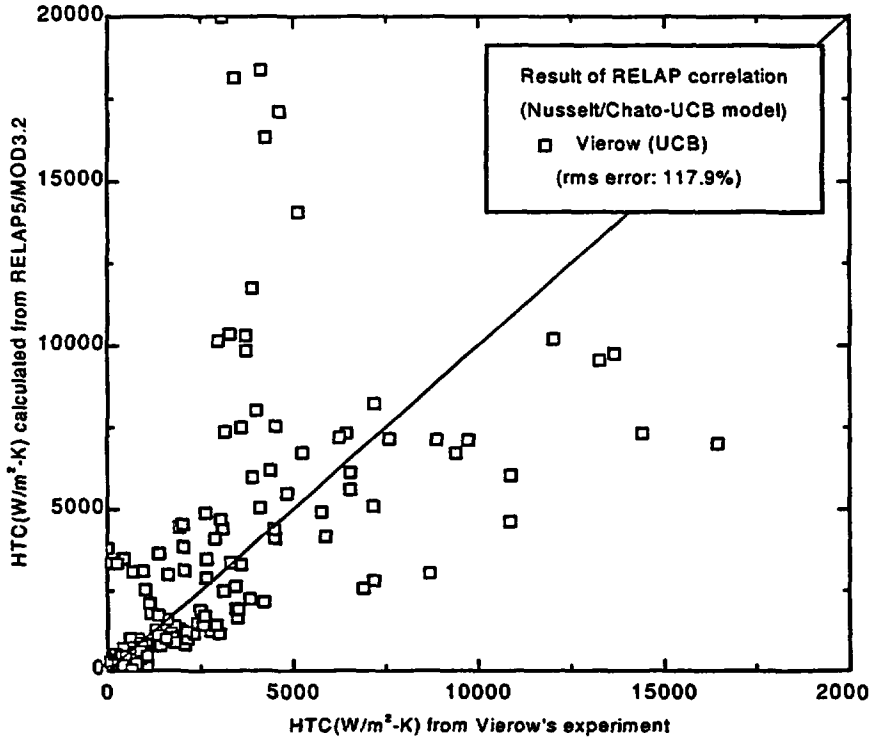

Figure 3.4: Assessment of alternative model of RELAP5/MOD3.2 with steam-air experimental data

The UCB multiplication factors in the alternative model are developed based on the Vierow's experimental data[9]. As Vierow's experimental data used for the development of the UCB multiplier in the alternative model show great scattering as shown in Figure 3.4, it is desirable to develop a better correlation with a larger data pool.

Figure 3.5 shows the assessment results for the alternative model of RELAP5/MOD3.2 with the steam-helium experimental data by Hasanein[14] and Kuhn[16]. As the enhancement factor, f_1, is always overestimated, the model predicts higher values than both Hasanein's and Kuhn's experimental data.The difference between Kuhn's data and Hasanein's data is from the difference between their experimental conditions. As Hasanein's experiments are performed over a range of low mixture Reynolds number compared with the Kuhn's exper-

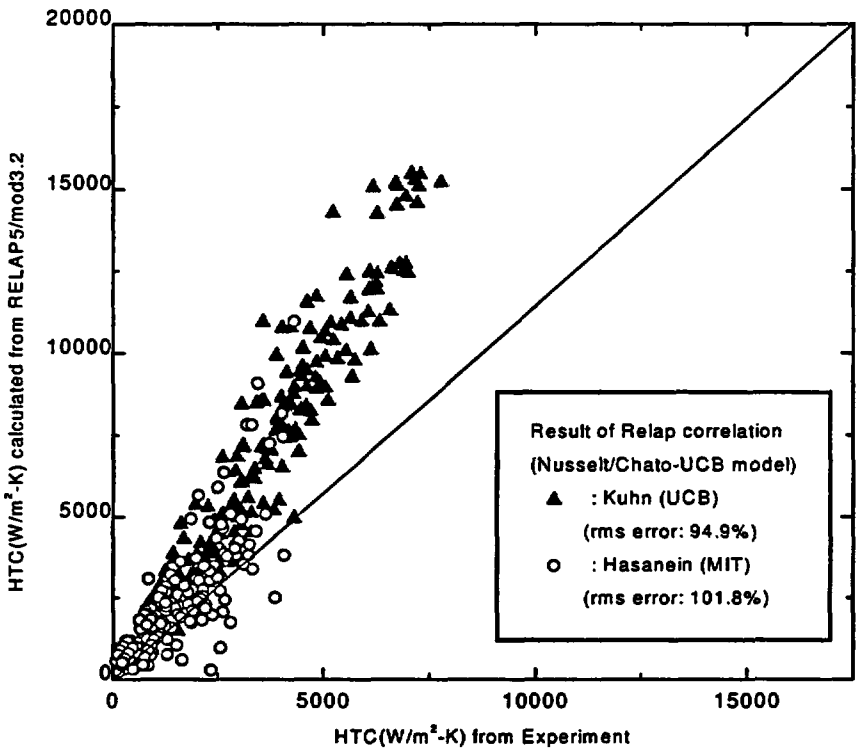

Figure 3.5: Assessment of alternative model of RELAP5/MOD3.2 with steam-helium experimental data

imental data, most of his data have low heat transfer coefficients and its correlation gives better prediction on the data with low mixture Reynolds number.

3.3 RELAP5/MOD3.2 Nodalization

The nodalization scheme of the RELAP5/MOD3.2 code of the present experimental facility is shown in Figure 3.6.

The present RELAP5/MOD3.2 nodalization used for this simulation contains 41 control volumes, 6 junctions, a valve and a heat structure.

Time-dependent volumes acting as infinite sources or sinks are used to represent boundary conditions both for the steam-noncondensable gas mixture flow in a condensing tube and for

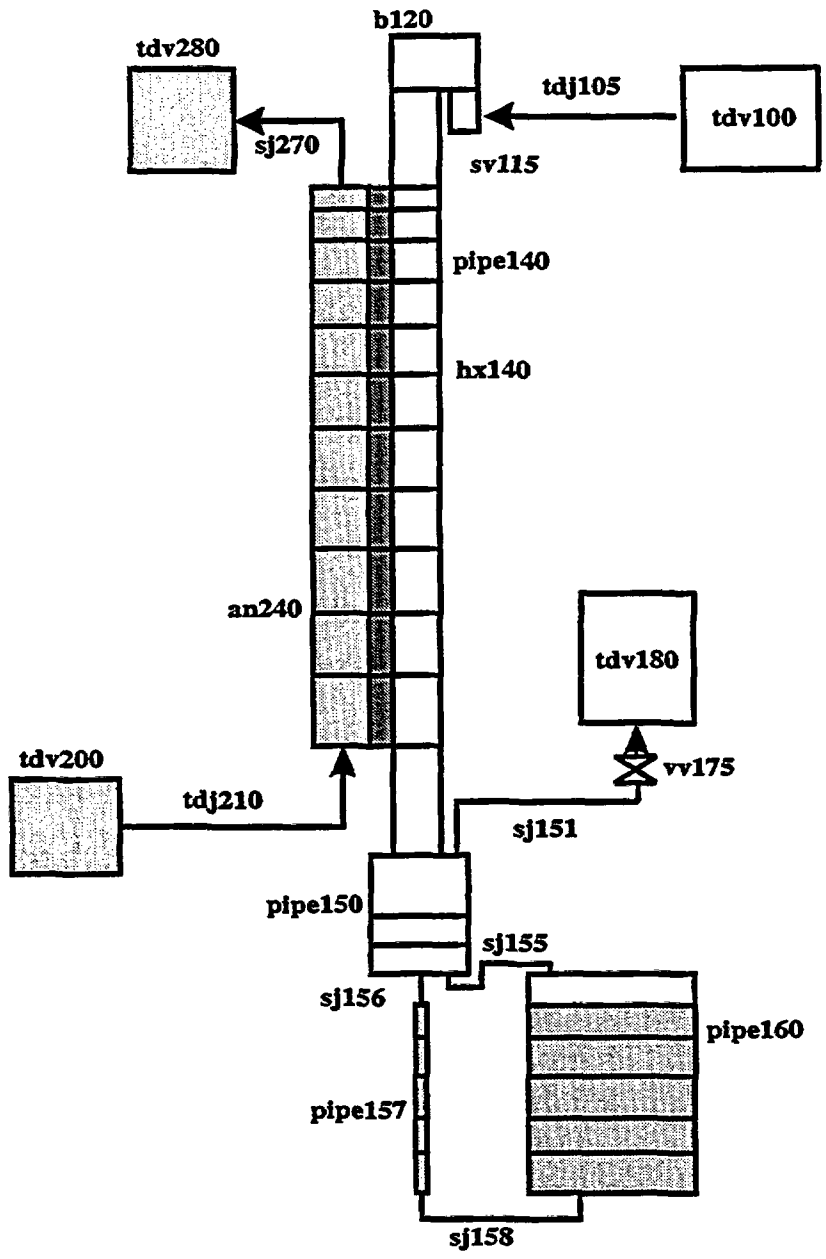

Figure 3.6: Nodalization scheme of the RELAP5/MOD3.2 code for PCCS experimental facility

the coolant flow in a coolant jacket. For the simulation of the coolant jacket, two time dependent volumes 200 and 280 are connected to the annulus 240 with 11 volumes via a time dependent juction 210 and a single junction 270. Similarly, for the simulation of the steam-noncondensable gas mixture flow, two time dependent volumes 100 and 180, a pipe with 13 volumes, a time dependent juction 105 and a single juntion 151 are also used.

A branch 120 is used to simulate an upper plenum and three pipe volumes 150, 160 and 157 are used to simulate a lower plenum, a drain tank and a connecting pipe between the lower plenum and the drain tank, respectively. The above three pipes are connected using single junctions 155, 156 and 158. A valve 175 is used to regulate the venting of the mixture of the residual steam and the noncondensable gas.

A heat structure 140 with 11 volumes is used to represent the heat transferred from the steam-noncondensable gas mixture to the coolant through the condensing tube.

3.4 Simulation Results and Discussion

3.4.1 Base case calculation

For base case calculations, five sub-tests are simulated by RELAP5/MOD3.2. As listed in Table 3.2, the following 7 input parameters are varied: the pressure at the inlet of the test section, P_{in}; its temperature, T_{in}; the inlet steam-air mixture flow rate, MF; the inlet air mass fraction, AMF; the temperature at the outlet of the test section, T_{out}; the temperature at the inlet of the coolant, $T_{c,in}$; the coolant flow rate, CF.

Steady state calculations were performed to determine whether or not it can describe properly the steam condensation experiments in the presence of noncondensables in a vertical tube of PCCS. These simulations used both the default model and the alternative model of the RELAP5/MOD3.2 code to be compared each other.

Table 3.2: Input parameters for base case calculations

Exp. No.	P_{in} (kpa)	T_{in} $(°C)$	MF (kg/h)	AMF (%)	T_{out} $(°C)$	$T_{c,in}$ $(°C)$	CF (gpm)
4d	281.3	129.0	32.8	10.2	62.3	16.4	2.4
11d	239.9	121.4	21.3	20.0	81.1	28.9	2.4
12a	463.2	140.4	18.4	30.1	66.6	28.7	2.4
12b	465.5	143.4	32.7	21.5	81.6	29.3	2.4
13b	185.4	110.5	18.2	30.3	81.7	28.4	2.4

Comparison of two simulation results with experimental data

Two simulation results of each steady state calculation were compared with each other, and they were also compared with the experimental data. Two simulation results with different condensation models were compared with the experimental data of *E13b* in Figures 3.7 through 3.12.

The following main characteristics are found:

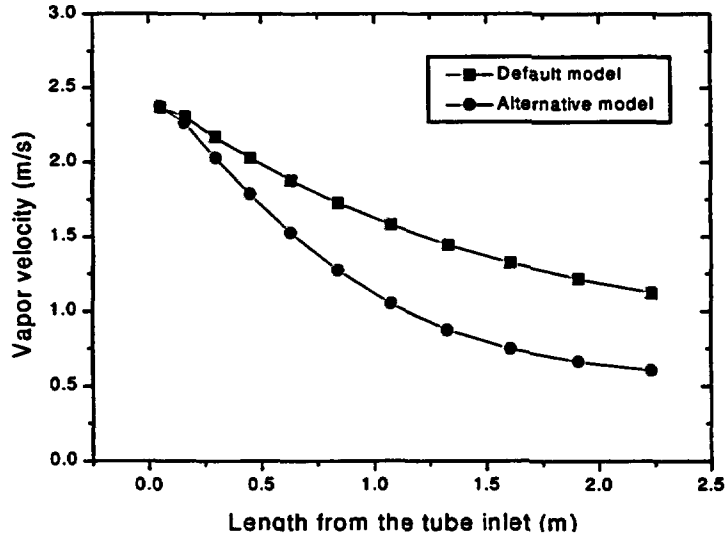

Figure 3.7: Comparison of steam velocities calculated using two condensation models with the experimental data of *E13b*

- As shown in Figure 3.7, the calculated steam velocity from the default model is always higher than that from the alternative model. They begin to condense with the same inlet velocities at the inlet, but the local steam velocity calculated from the default model decreases more slowly than that from the alternative model. As the amount of the mass transferred to the liquid film by the steam condensation is large for the simulation using the alternative model, the steam flow rate is calculated to be smaller for the alternative model than for the default model.

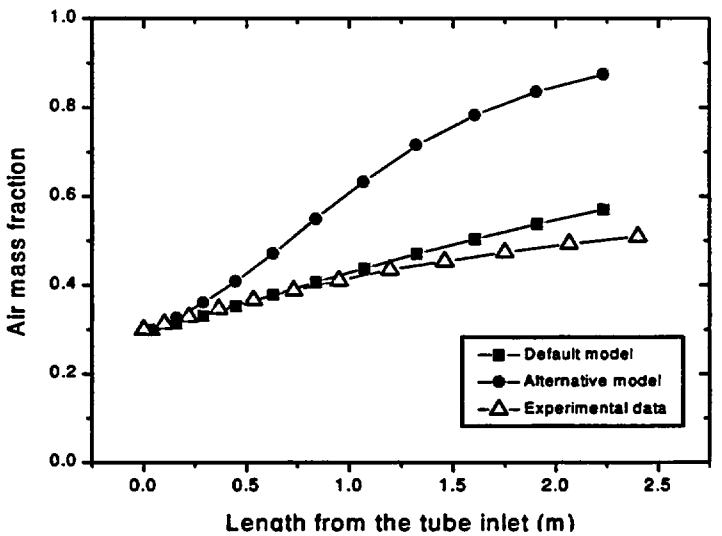

Figure 3.8: Comparison of air mass fractions calculated using two condensation models with the experimental data of *E13b*

- As shown in Figure 3.8, the calculated air mass fraction from the default model is always lower than that from the alternative model. The calculated air mass fraction from the default model increases linearly and is always slightly higher than the experimental data. However the calculated air mass fraction from the alternative model increases rapidly in the upper part of the condensing tube and the inclination is decreased in the lower part, it always keeps higher value than the experimental data except for the inlet.

- Figure 3.9 shows the distributions of the mixture bulk, the saturated steam, the inner

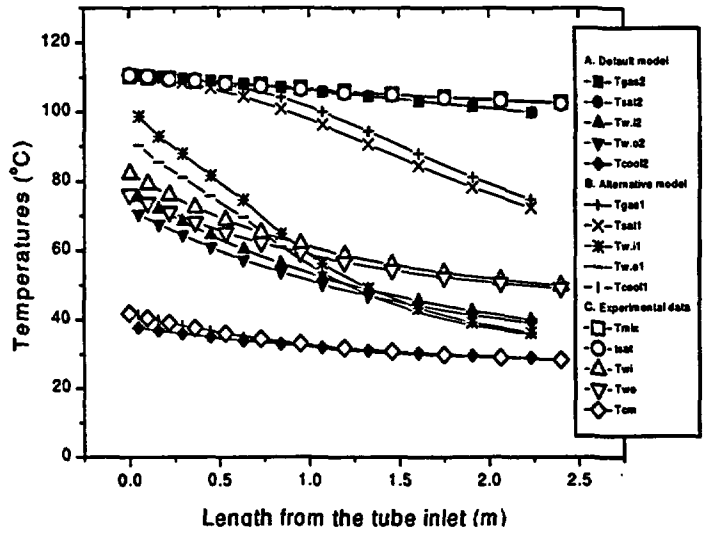

Figure 3.9: Comparison of temperatures calculated using two condensation models with the experimental data of *E13b*

and the outer tube wall and the coolant bulk temperatures along the condensing tube. All the calculated temperatures from the default model decrease more slowly than those from the alternative model. So the mixture bulk temperature from the default model always keeps a higher value than that from the alternative model, and its coolant bulk temperature always keeps a lower value. Most of the inner and the outer wall temperatures from the default model keep lower values than those from the alternative model except for the outlet of the condensing tube. The experimental mixture bulk temperature is always similar to that from the default model. The experimental inner and outer wall temperatures keep lower values than those from both the default model and the alternative model, but they crossed with each other in the upper part of the condensing tube. The experimental coolant bulk temperature goes between that from the default model and that from the alternative model along the condensing tube.

- As shown in Figure 3.10, the calculated coolant-side heat transfer coefficient from the default model is lower than that from the alternative model in the upper region of

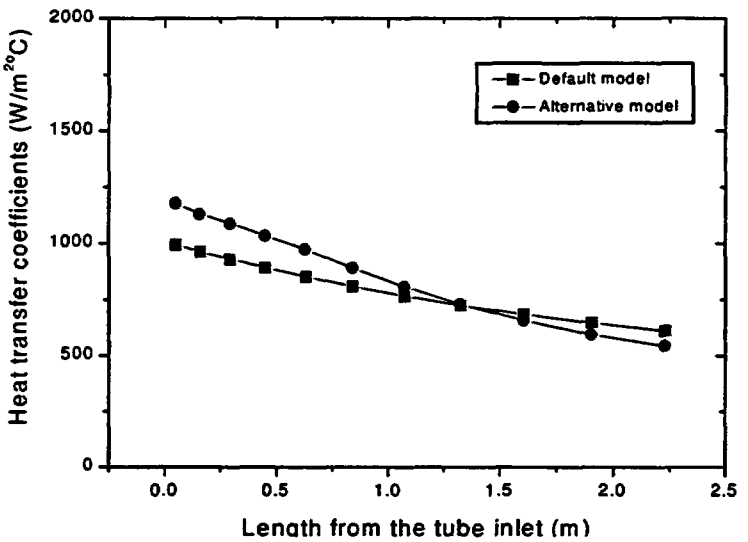

Figure 3.10: Comparison of coolant side heat transfer coefficients calculated using two condensation models with the experimental data of *E13b*

the condensing tube, but the tendency is opposite in the lower part of the condensing tube. The change of the simulated results in the coolant side has little effect on the condensation heat transfer characteristics in a condensing tube. Sometimes the rapid increase of the simulated one from the alternative model is due to the change of the heat transfer characteristics from the single phase convective mode to the two phase boiling mode near the inlet of the condensing tube.

- As shown in Figure 3.11, the calculated heat flux from the default model is always lower than that from the alternative model in the upper region of the condensing tube, and they are similar in the lower region. The condensation heat flux calculated from the default model is always much lower than the experimental data throughout the condensing tube. However, the condensation heat flux calculated from the alternative model is a little higher than the experimental data in the upper region of the condensing tube, and they crossed each other in the middle of the condensing tube.

- As shown in Figure 3.12, the calculated condensation heat transfer coefficient from the

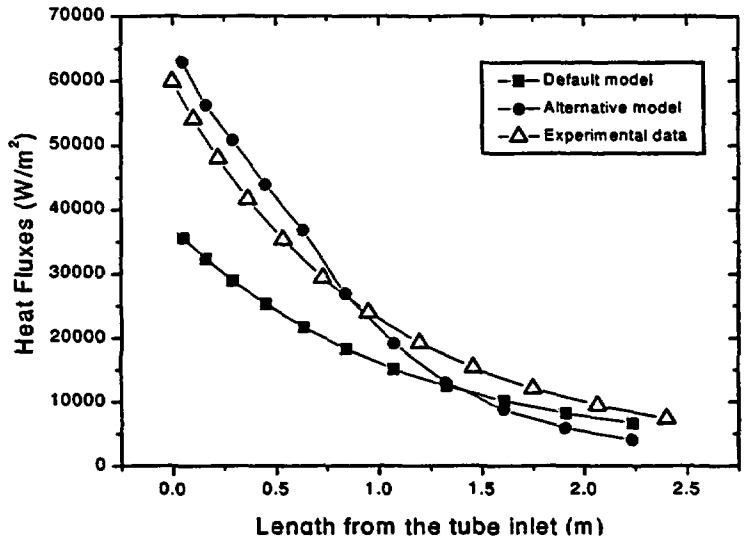

Figure 3.11: Comparison of heat fluxes calculated using two condensation models with the experimental data of *E13b*

default model is always lower than that from the alternative model throughout the condensing tube. Similar to the comparison results of the heat flux, the calculated heat transfer coefficient from the default model is always lower than the experimental data, while the calculated one from the alternative model is always higher than the experimental data. Three heat transfer coefficients, or two simulated results and one experimental data, are greatly different in the inlet of the test section, but they are similar in the outlet of the condensing tube, where the amount of steam is greatly reduced by condensation and the convective heat transfer is dominant.

Several simulation results for experiments with different initial condition

From experimental studies, it is known that the main parameters controlling the condensation with noncondensables in a vertical tube are the inlet steam-air mixture flow rate, the inlet air mass fraction, and the inlet saturated steam temperature. Simulations on experiments are performed to show the parametric effects with both the default model and the alternative

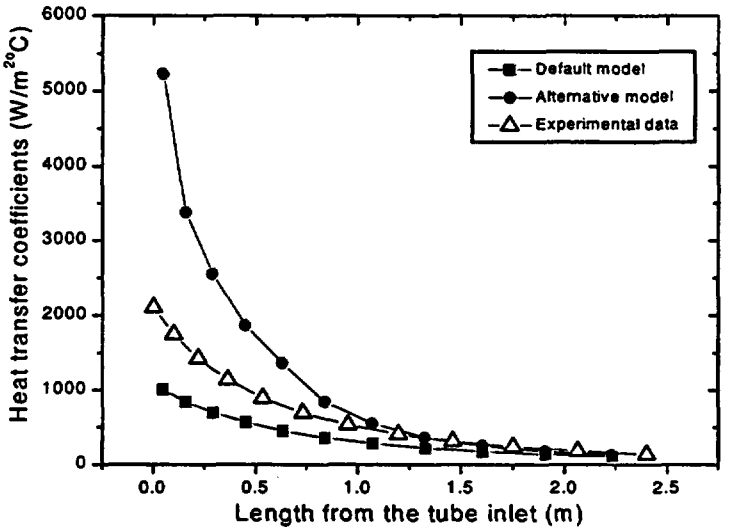

Figure 3.12: Comparison of condensation heat transfer coefficients calculated using two condensation models with the experimental data of *E13b*

model of RELAP5/MOD3.2, and they are compared with the experimental data.

The following main characteristics are found :

- Figure 3.13 and 3.14 show simulations for experiments *E12a* and *E11d*, respectively. Those two experiments have high inlet air mass fractions above 10% and low inlet steam-air mixture flow rates below $30kg/hr$. The simulated heat transfer coefficient using the alternative model is always higher than that using the default model in the upper part of the condensing tube, and they are approaching along the condensing tube to give similar values in the lower part. The heat transfer coefficient calculated from the default model is always lower, but that from the alternative model is higher than the experimental data.

- Figure 3.15 shows simulation for experiments *E12b*, which was performed for relatively high inlet steam-air mixture flow rate above $30kg/hr$. The calculated heat transfer coefficient from the alternative model becomes similar to the experimental data both at the inlet and the outlet of the condensing tube, but it is higher than the experimental

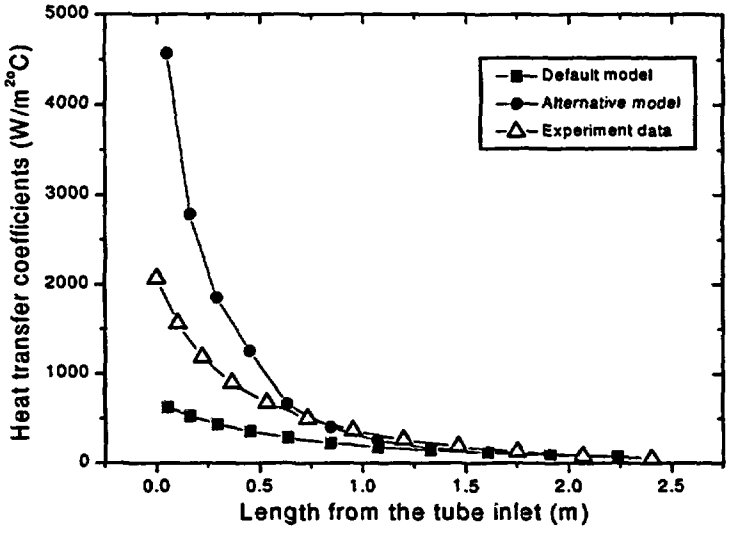

Figure 3.13: Comparison of condensation heat transfer coefficients calculated using two condensation models with the experimental data of *E12a*

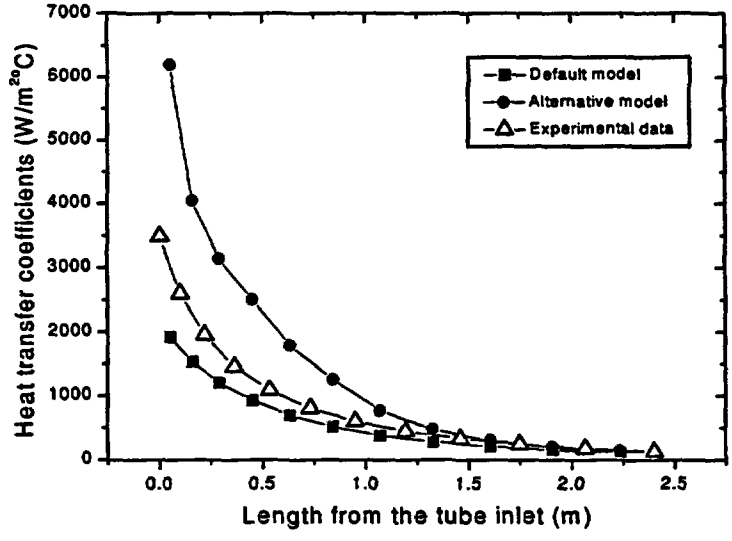

Figure 3.14: Comparison of condensation heat transfer coefficients calculated using two condensation models with the experimental data of *E11d*

data in the middle of the condensing tube. The heat transfer coefficient calculated using the default model is lower than the experimental data in the inlet, and they are approaching along the condensing tube to give similar values in the lower part. This tendency of the default model is unchanged regardless of the change of the inlet mixture flow rate.

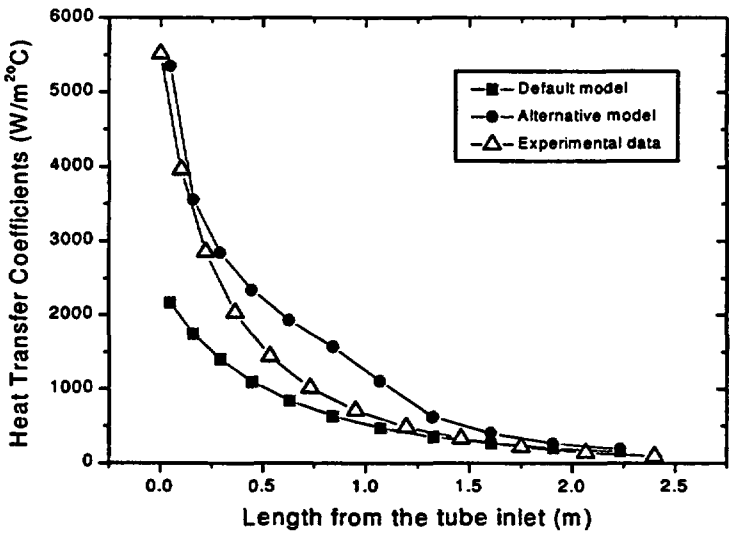

Figure 3.15: Comparison of condensation heat transfer coefficients calculated using two condensation models with the experimental data of *E12b*

- Figure 3.16 shows simulation for experiments *E4d*, which was performed for relatively high inlet steam-air mixture flow rate above $30kg/hr$ and low inlet air mass fraction below 10%. Similar to the case of high inlet mixture flow rate above $30kg/hr$, the calculated heat transfer coefficient from the alternative model becomes similar to the experimental data both at the inlet and the outlet of the condensing tube, but it predicts higher values in the middle of the condensing tube. This tendency of the alternative model is unchanged regardless of the change of the inlet air mass fraction. The heat transfer coefficient calculated using the default model simulates well the experimental data throughout the condensing tube. $30kg/hr$ and low inlet air mass fraction below

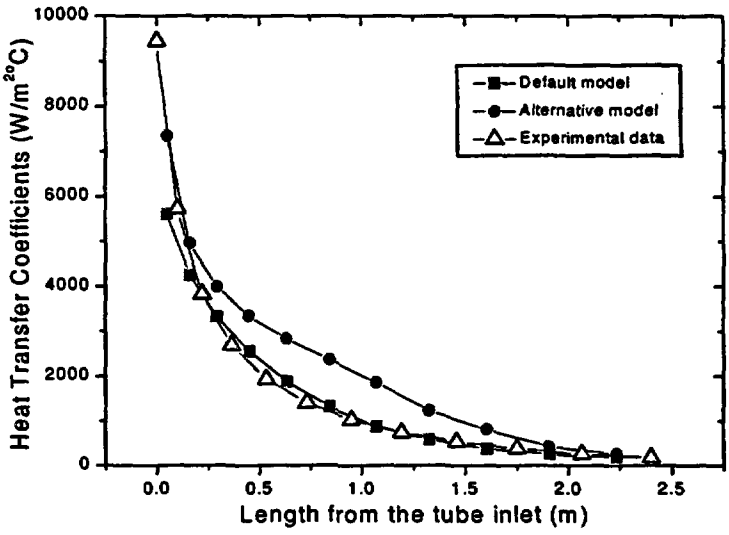

Figure 3.16: Comparison of condensation heat transfer coefficients calculated using two condensation models with the experimental data of *E4d*

10%

- When the inlet steam-air mixture flow rate is low below $30kg/hr$ and the inlet air mass fraction is high above 10%, both the default model and the alternative model predict wrong, and they are needed to be improved. With the increase of the mixture flow rate, the default model predicts wrong except for the outlet of the condensing tube, while the alternative model predicts correctly both in the inlet and outlet, but it also over-predicts the heat transfer coefficient in the middle of the condensing tube. For the condition of relatively low inlet air mass fraction below 10% and high inlet mixture flow rate above $30kg/hr$, the default model predicts well the experimental data. It is considered to be that the effect of the inlet steam-air mixture flow rate is not properly considered in the default model, and the effect of the inlet air mass fraction in the alternative model.

3.4.2 Nodalization study

The RELAP5/MOD3.2 code permits the user to vary the nodalization. By changing the number of nodes in the heat structure, it is possible to investigate whether or not the node number affects the heat transfer characteristics in the RELAP5/MOD3.2 code. It is known that the change of the number of the divided nodes has little influence on the simulation results of the condensation phenomena with RELAP5/MOD3.2. The sub-program *conden.f* is based on the film thickness to make it a local form instead of the average value used in RELAP5/MOD3 up to MOD3.1.1.1 version. There was much effort to eliminate the dependence on the node size in condensation heat transfer coefficient for an inclined surface of RELAP5/MOD3.1[4].

To investigate this effect the test section tube is divided into 4, 8, 12, and 16 nodes regularly instead of the irregular 11 nodes in the base case calculation of *E12b*. The simulation is performed at the condition that the total pressure is $0.46547 Mpa$ and the inlet saturated steam temperature is $143.4^{o}C(416.55K)$. The calculated heat transfer coefficients vary almost the same along the condensing tube for the different node numbers, as shown in Figure 3.17. From the analysis of the simulated results it is concluded that the heat transfer characteristics both in the default and in the alternative model of RELAP5/MOD3.2 are little affected by the change of the node number in the heat structure.

3.4.3 Sensitivity study of input parameters

As listed in Table 3.3, input parameters are varied to compare the calculation results with changes of input parameters. The experiment *E12b* is selected as a base case. The effects of the coolant flow rate, the inlet coolant temperature, and the vented mixture temperature give negligible effects on the heat transfer coefficient in the condensing tube except for the minor variations due to the changes of the condition of the coolant. However, the inlet steam-air mixture flow rate, the inlet air mass fraction and the inlet saturated steam temperature give significant changes of the heat transfer coefficient in the condensing tube. In this section,

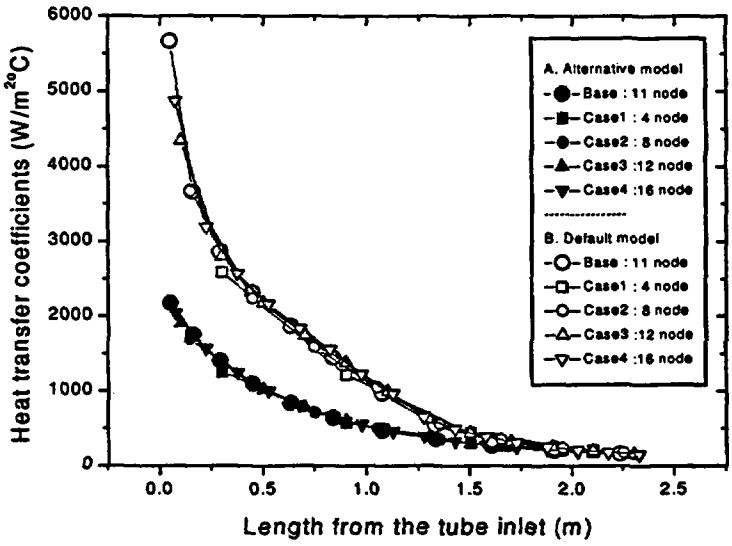

Figure 3.17: Comparison of calculated heat transfer coefficients with the variation of the node number

three important parameters are changed to show their sensitivity.

Simulations are performed for each case with two wall film condensation models, the default model and the alternative model. The difference of heat transfer coefficients is decreased between two simulation results, as the inlet steam-air mixture flow rate increases, the inlet air mass fraction decreases, and the inlet saturated steam temperature decreases. The heat transfer coefficient calculated using the alternative model is always higher than that using the default model, especially in the inlet of the condensing tube. It is due to the fact that the correlation of the alternative model is based on the film thickness, which is very thin in the inlet.

Effects of inlet steam-air mixture flow rate

The inlet steam-air mixture flow rate varies between 10, 20, 40, and $50kg/hr$ instead of the $33kg/hr$ of the base case.

Figures 3.18 and 3.19 show the simulation results of local air mass fraction along the condensing tube with the change of the inlet steam-air mixture flow rate at the condition

Table 3.3: Input parameters for the sensitivity study

I.D.	Node Number	P_{in} (kpa)	T_{in} $(°C)$	MF (kg/h)	AMF (%)	T_{out} $(°C)$	$T_{c,in}$ $(°C)$	CF (gpm)
ss0	42	465.5	143.4	32.7	21.5	81.6	29.3	2.4
nd1	35	465.5	143.4	32.7	21.5	81.6	29.3	2.4
nd2	39	465.5	143.4	32.7	21.5	81.6	29.3	2.4
nd3	43	465.5	143.4	32.7	21.5	81.6	29.3	2.4
nd4	47	465.5	143.4	32.7	21.5	81.6	29.3	2.4
sf1	42	465.5	143.4	10.0	21.5	81.6	29.3	2.4
sf2	42	465.5	143.4	20.0	21.5	81.6	29.3	2.4
sf3	42	465.5	143.4	40.0	21.5	81.6	29.3	2.4
sf4	42	465.5	143.4	50.0	21.5	81.6	29.3	2.4
af1	42	403.9	143.4	32.7	2.5	81.6	29.3	2.4
af2	42	410.5	143.4	32.7	5.0	81.6	29.3	2.4
af3	42	425.0	143.4	32.7	10.0	81.6	29.3	2.4
af4	42	562.3	143.4	32.7	40.0	81.6	29.3	2.4
st1	42	118.3	100.0	32.7	21.5	81.6	29.3	2.4
st2	42	197.3	115.0	32.7	21.5	81.6	29.3	2.4
st3	42	315.3	130.0	32.7	21.5	81.6	29.3	2.4
st4	42	555.6	150.0	32.7	21.5	81.6	29.3	2.4

which the other parameters are the same with the base case, using both the default model and the alternative model, respectively. The local air mass fraction of the default model is linearly increased along the condensing tube keeping a relatively low air mass fraction compared with that of the alternative model, which varies greatly along the condensing tube especially for the low inlet steam-air mixture flow rate.

Figures 3.20 and 3.21 show the simulation results of local heat transfer coefficient, using both the default model and the alternative model, respectively. For the simulation using the default model, the local heat transfer coefficient is increased throughout the condensing tube with the increase of the inlet steam-air mixture flow rate, and it is much more increased especially in the inlet. However, for the simulation using the alternative model, it is independent of the inlet steam-air mixture flow rate in the inlet of the tube, but it is very much changed in the middle of the condensing tube.

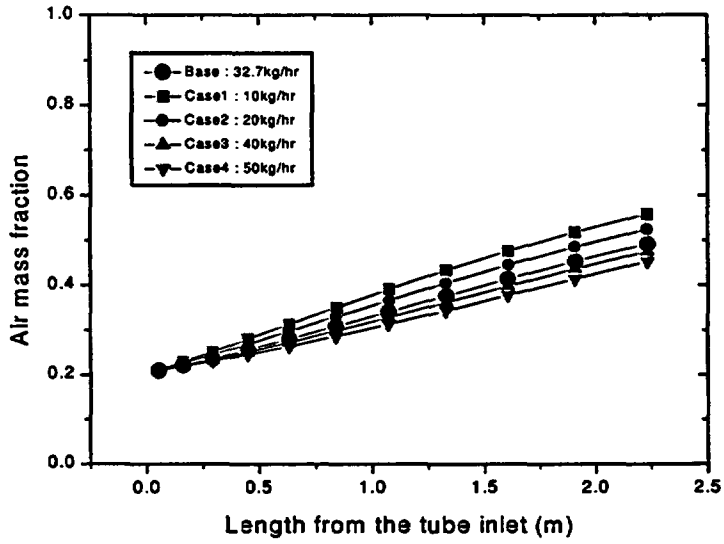

Figure 3.18: Comparison of calculated air mass fractions with the variation of the steam-air mixture flow rate in default model

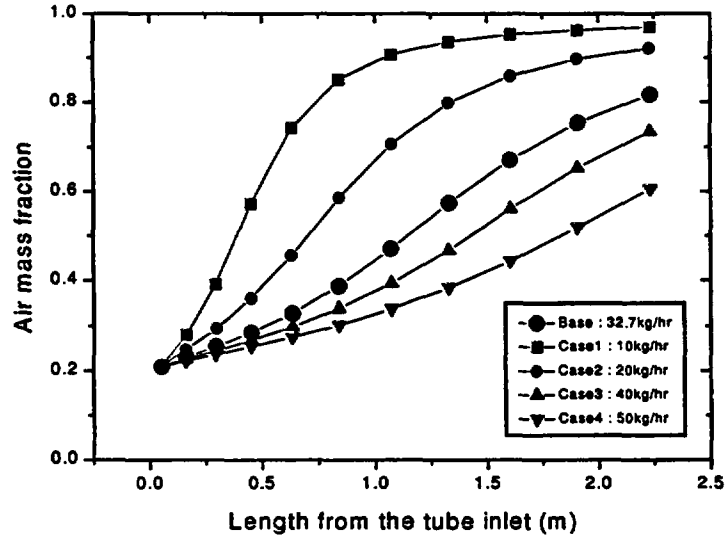

Figure 3.19: Comparison of calculated air mass fractions with the variation of the steam-air mixture flow rate in alternative model

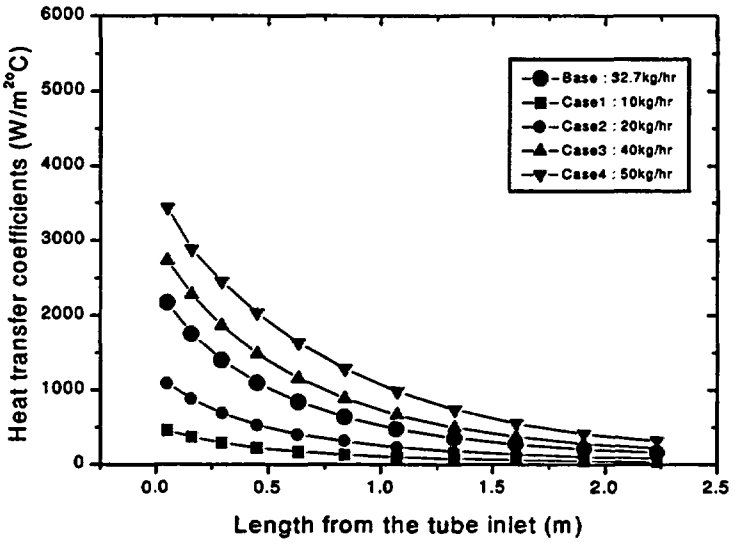

Figure 3.20: Comparison of calculated heat transfer coefficients with the variation of the steam-air mixture flow rate in default model

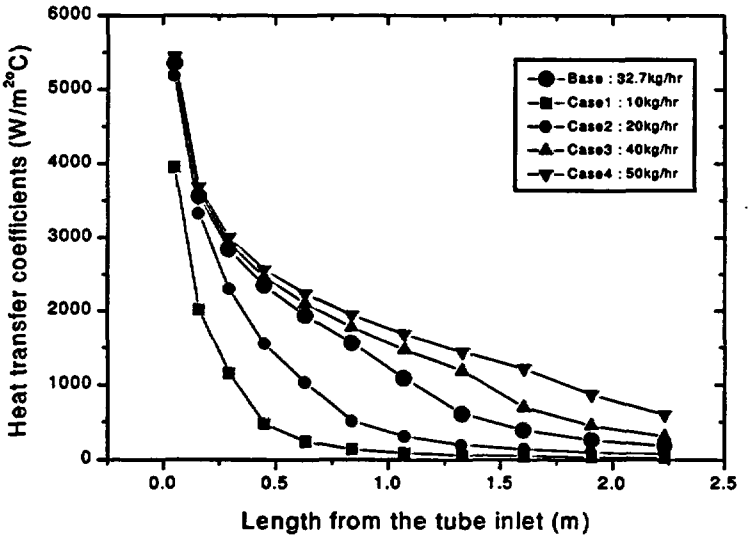

Figure 3.21: Comparison of calculated heat transfer coefficients with the variation of the steam-air mixture flow rate in alternative model

The two simulated heat transfer coefficients are greatly different in the inlet, but they are similar in the outlet of the condensing tube. As the inlet mixture flow rate increases, the heat transfer coefficient using the default model increases to be similar with that using the alternative model. Particularly with the low steam flow rate, the simulated heat transfer coefficients by the alternative model is more highly evaluated than that by the default model.

Effects of inlet air mass fraction

The inlet air mass fraction varies between 2.5, 5, 10, and 40% instead of the 20% of the base case.

Figures 3.22 and 3.23 show the simulation results of local air mass fraction along the condensing tube with the change of the inlet air mass fraction at the condition which the other parameters are the same with the base case, using both the default model and the alternative model, respectively. The local air mass fraction of the default model is linearly increased along the condensing tube keeping a relatively low air mass fraction compared with that of the alternative model, which varies greatly along the condensing tube, especially for the low inlet air mass fraction.

Figures 3.24 and 3.25 show the simulation results of local heat transfer coefficient, using both the default model and the alternative model, respectively. For the simulations using both the default model and the alternative model, the heat transfer coefficients are highly decreased in the inlet of the condensing tube with the increase of the air mass fraction, but they become similar in the outlet. However, the heat transfer coefficient calculated using the default model is always lower than that using the alternative model except for the lower part of the condensing tube. The effect of inlet air mass fraction is shown only in the upper part of the condensing tube, but it is negligible in the lower part.

Effects of inlet saturated steam temperature

The inlet saturated steam temperature varies between 100, 115, 130, and $150^{o}C$ instead of the $143^{o}C$ of the base case.

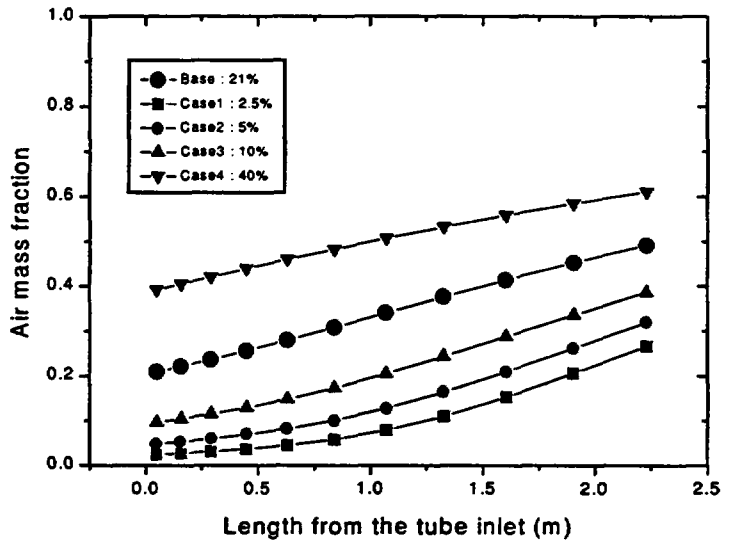

Figure 3.22: Comparison of calculated air mass fractions with the variation of the inlet air mass fraction in default model

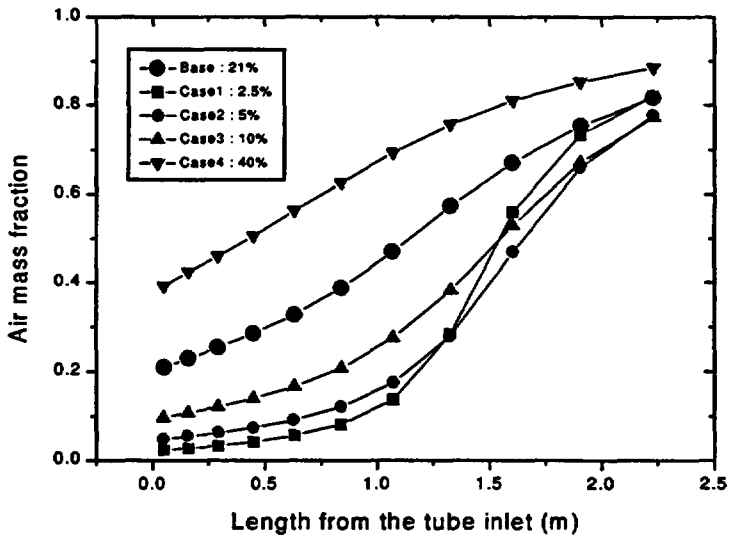

Figure 3.23: Comparison of calculated air mass fractions with the variation of the inlet air mass fraction in alternative model

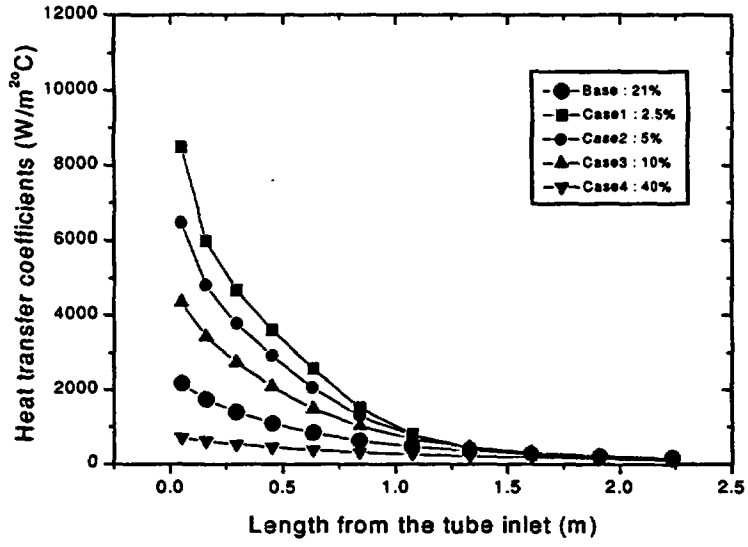

Figure 3.24: Comparison of calculated heat transfer coefficients with the variation of the inlet air mass fraction in default model

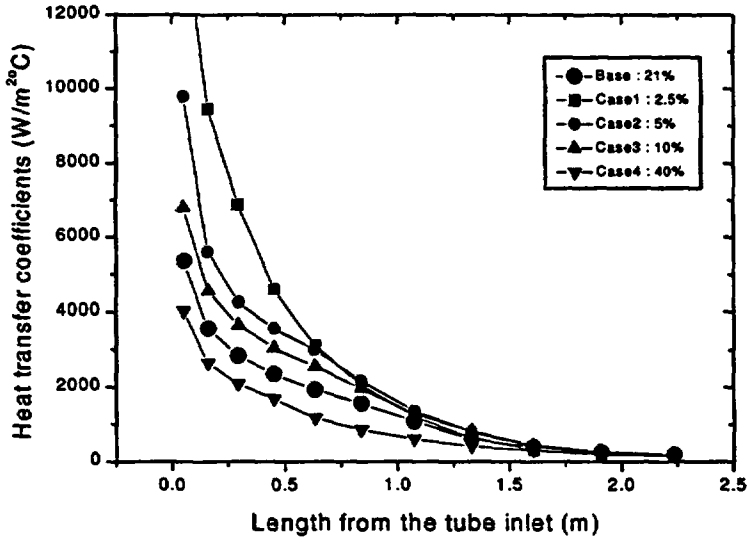

Figure 3.25: Comparison of calculated heat transfer coefficients with the variation of the inlet air mass fraction in alternative model

Figures 3.26 and 3.27 show the simulation results of local air mass fraction along the condensing tube with the change of the inlet saturated steam temperature at the condition which the other parameters are the same with the base case, using both the default model and the alternative model, respectively. The local air mass fraction of the default model is linearly increased along the condensing tube keeping a relatively low air mass fraction compared with that of the alternative model, which varies greatly along the condensing tube especially for the high inlet saturated steam temperature.

Figures 3.28 and 3.29 show the simulation results of local heat transfer coefficient, using both the default model and the alternative model, respectively. For the simulation using the default model, the heat transfer coefficient is highly decreased with the increase of the inlet saturated steam temperature in the inlet of the condensing tube, but it is little changed in the outlet. However, for the simulation using the alternative model, the heat transfer coefficient is a little decreased with the increase of the inlet saturated steam temperature in the upper part of the condensing tube, but it is much more decreased in the lower part.

3.4.4 Run statistics

The computer used in the calculation is a SUN SPARC 10 with SunOS 4.1.3-KL operating system. The random access memory is $32Mbyte$, the calculation speed is $86.1MIPS$, and the clock speed of CPU is $36MHz$.

The CPU time, the time step size, and the grind time were compared between two calculation results with different wall film condensation models. Figure 3.30 shows the required CPU times with respect to the real problem time for the base case calculation of *E12b*. The required CPU times increase linearly for both the default model and the alternative model, except for the initial transient situation. The CPU time is greatly changed near $40sec$. When the default model is used, the required CPU time is slightly longer than that of the alternative model. Figure 3.31 shows the time step sizes with respect to the real problem time for the base case calculation of *E12b*. The time steps fluctuate between 0.0125, 0.025, and 0.05sec for both the default model and the alternative model. When the default condensation model

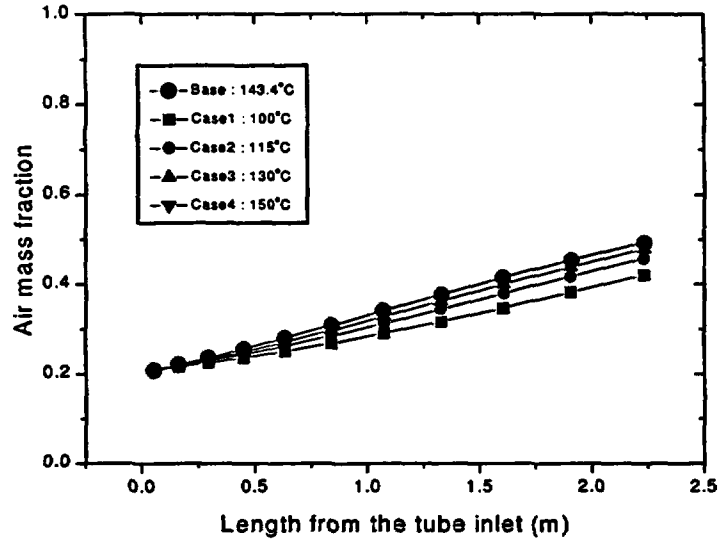

Figure 3.26: Comparison of calculated air mass fractions with the variation of the inlet saturated temperature in default model

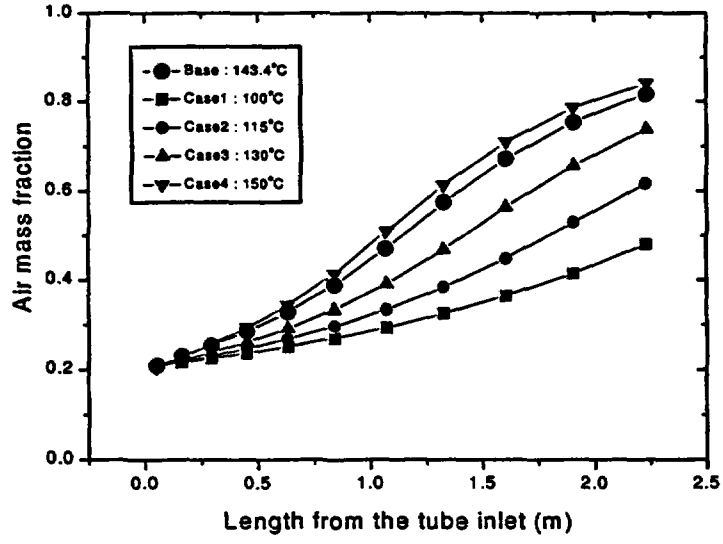

Figure 3.27: Comparison of calculated air mass fractions with the variation of the inlet saturated temperature in alternative model

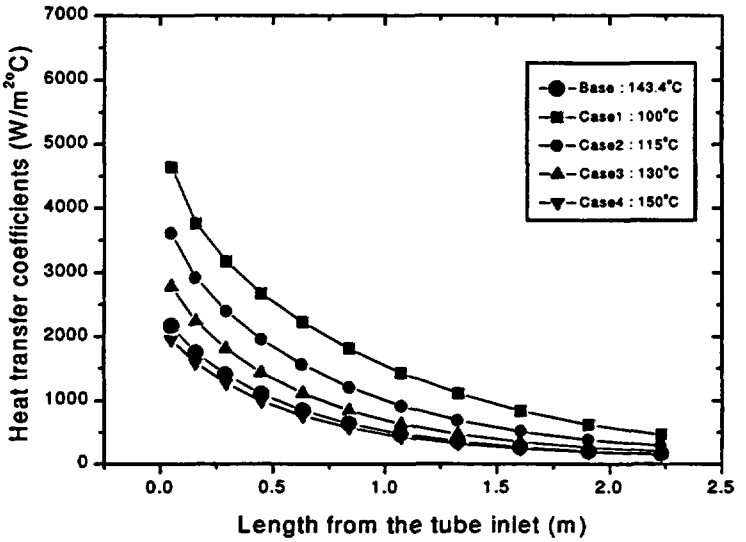

Figure 3.28: Comparison of calculated heat transfer coefficients with the variation of the inlet saturated temperature in default model

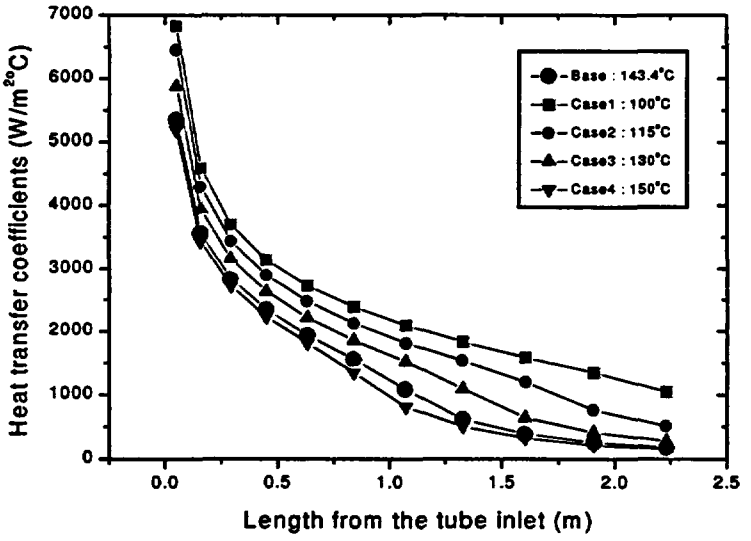

Figure 3.29: Comparison of calculated heat transfer coefficients with the variation of the inlet saturated temperature in alternative model

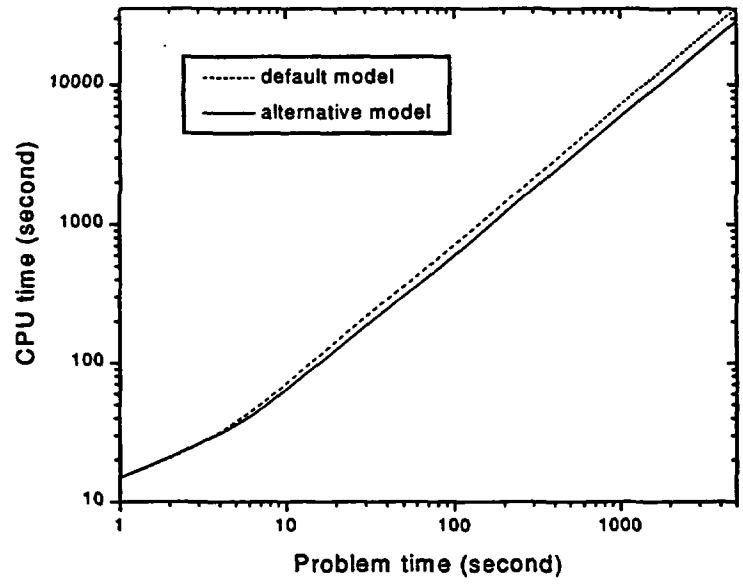

Figure 3.30: Comparison of required CPU times of two condensation models

is used, the time step size is smaller, and its fluctuation is more frequent than that of the alternative model.

The time step determined by the code is also shown in Figure 3.32 with respect to the user specified maximum time step for the base calculation of *E12b*. The code determined time step with the default model is observed to scatter much more than that with the alternative model. It validates larger fluctuation of the time step and longer required CPU time.

The grind time is expressed as:

$$Grind\ time = \frac{CPU \times 10^3}{C \times \Delta T} \tag{3.14}$$

where CPU is the CPU time, C is the total number of model volumes, and ΔT is the number of time steps. It means the CPU time used for calculating a volume during a second.

Table 3.4 shows the required CPU time and the grind time for the base case calculations, and Table 3.5 shows those for the nodalization study and the sensitivity study.

The required CPU time is the highest when the inlet mixture flow rate is the highest and

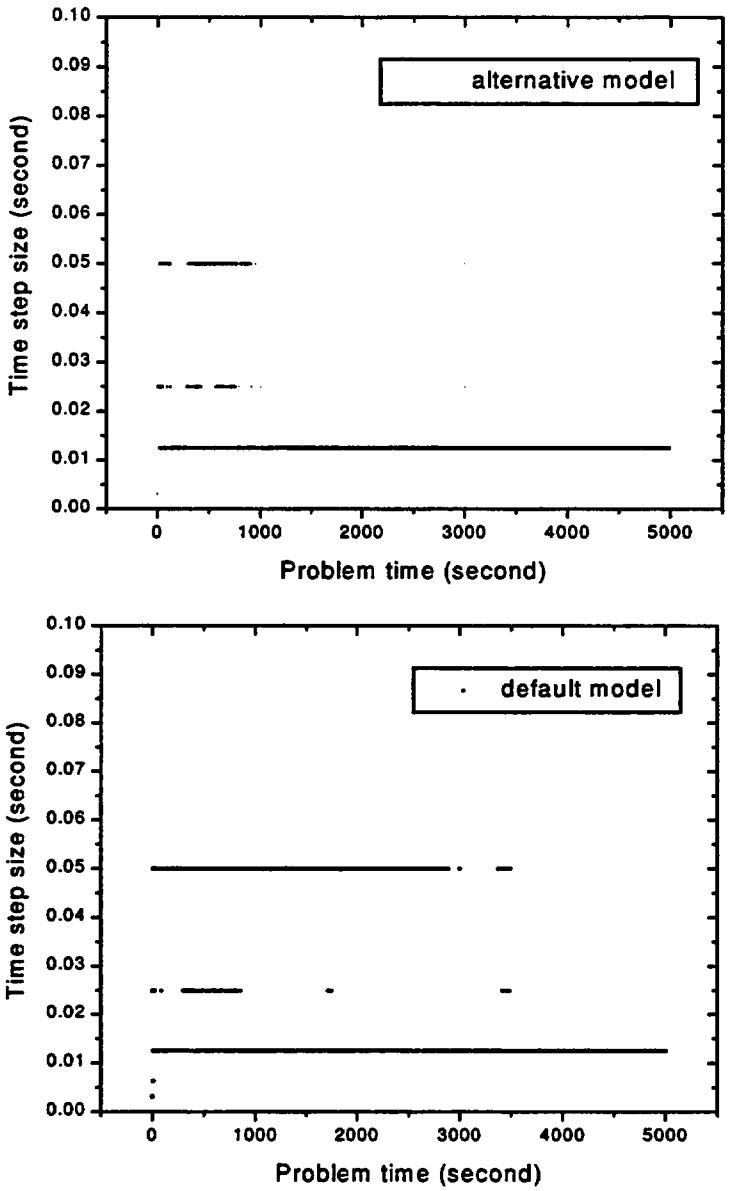

Figure 3.31: Comparison of time step sizes of two condensation models

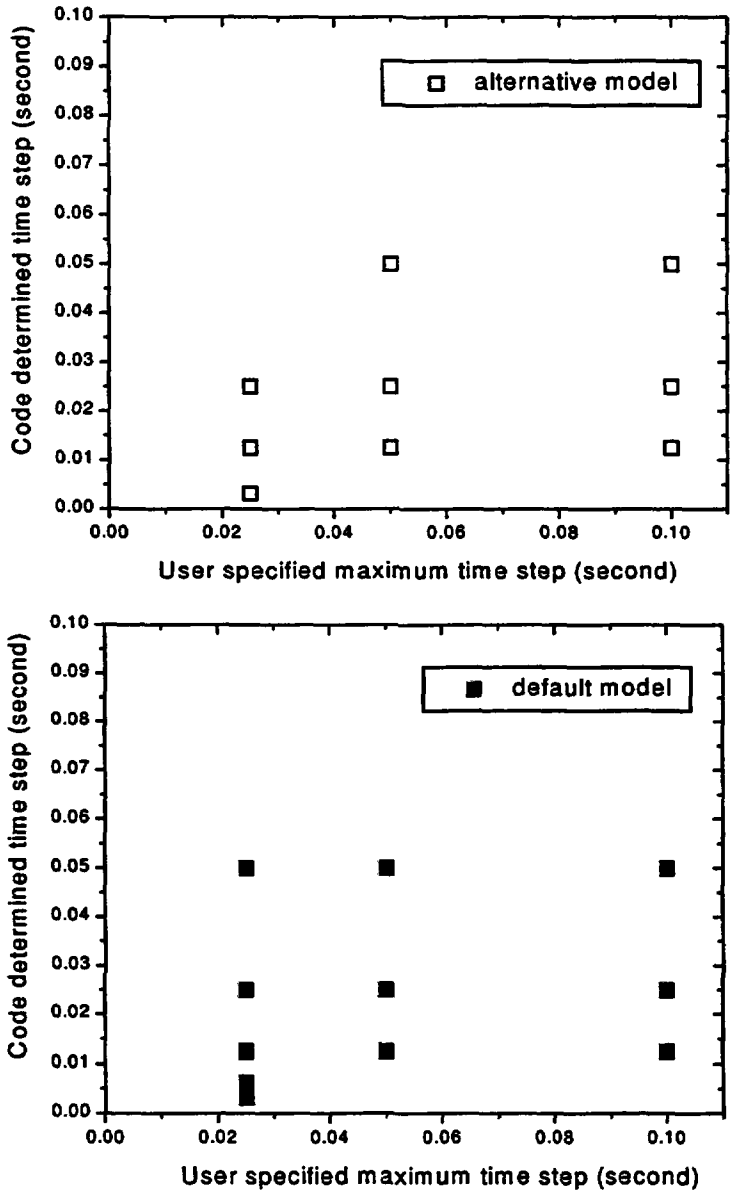

Figure 3.32: Comparison of code determined time steps of two condensation models

both the air mass fraction and the inlet saturated steam temperature is the lowest. The grind time of the default model is about 23% higher than that of the alternative model. The grind time is a little increased when more volumes are included in RELAP5/MOD3.2 simulation, but it is little changed with the same node number when the other parameters are changed.

Table 3.4: The CPU time and the grind time of the simulation of KAIST condensation experiment

I.D.	Problem time (second)	condensation model	CPU time (second)	Number of time step	Grind time
4d	1000	alternative	7320.5	61748	2.823
		default	8740.3	60302	3.451
11d	1000	alternative	7178.6	59666	2.865
		default	8986.4	59942	3.569
12a	1000	alternative	3434.6	28177	2.902
		default	4286.2	28326	3.603
12b	1000	alternative	5944.8	46591	3.038
		default	7202.1	46671	3.674
	5000	alternative	28519.5	233309	2.910
		default	35098	233281	3.582
13b	1000	alternative	7558.4	61716	2.916
		default	9902.7	66476	3.547

Table 3.5: The CPU time and the grind time of the sensitivity study

I.D.	Node	Problem time(s)	The alternative model			The default model		
			CPU time(s)	No. of time step	Grind time	CPU time(s)	No. of time step	Grind time
ss0	42	250	1511.6	11647	3.090	1790.1	11668	3.653
nd1	35	250	1053.1	11772	2.556	1127	11337	2.840
nd2	39	250	1380.8	12276	2.884	1576.7	12002	3.368
nd3	43	250	1680.6	12389	3.155	1928.8	11779	3.808
nd4	47	250	1862.7	11649	3.402	2289.8	11659	4.179
sf1	42	250	849.4	6854	2.951	728.7	4940	3.512
sf2	42	250	990.9	7995	2.951	1174.8	7903	3.539
sf3	42	250	1870.3	14974	2.974	2275.6	14843	3.650
sf4	42	250	2501.7	19888	2.995	3019.9	19850	3.622
af1	42	250	4463.4	36664	2.899	5415.8	36578	3.525
af2	42	250	3552.8	29639	2.854	4243.1	29052	3.477
af3	42	250	1997.7	16033	2.967	2307.2	15958	3.442
af4	42	250	1193.6	9369	3.033	1376.3	9094	3.603
st1	42	250	2587.1	19866	3.101	2364.7	15628	3.603
st2	42	250	1858.3	15328	2.887	2344.7	15276	3.655
st3	42	250	1863.4	15157	2.927	2302.4	15112	3.628
st4	42	250	1202	9728	2.942	1404.5	9593	3.486

Chapter 4

Conclusions and Recommendations

The capability of the RELAP5/MOD3.2 code in modeling the condensation heat transfer in the presence of noncondensable gas has been investigated. Several experiments are performed to get a reliable data on that condensation phenomena, to show the parametric effects on condensation heat transfer, and to elucidate the cause of data scattering among the previous experiments. With the constructed database direct assessments are carried out for both the default and alternative condensation models in RELAP5/MOD3.2. After the experimental apparatus being modeled with RELAP5/MOD3.2, the simulation results are compared between two wall film condensation models, and they are also compared with the experimental data. Nodalization study is performed to investigate the effect of the divided node number of the heat structure. Also the sensitivity study on the important experimental parameters is performed, and the run statistics are checked.

From the studies, the followings are concluded:

1. From the comparison of the experimental results, it is known that there are three important experimental parameters: the inlet steam-air mixture flow rate; the inlet air mass fraction; the inlet saturated steam temperature. The experimental results show that the condensation heat transfer coefficient increases as the inlet steam-air mixture flow rate increases, the inlet saturated steam temperature decreases, and the inlet air

mass fraction decreases.

2. From the direct assessment of two condensation models of RELAP5/MOD3.2, the default condensation model under-predicts the experimental data for the low heat transfer coefficient range, but it over-predicts the experimental data for the high heat transfer coefficient range. In case of the alternative condensation model, the predicted values are always higher than the experimental data.

3. When the two wall film condensation models of RELAP5/MOD3.2 are compared each other, the calculated air mass fraction from the default model is always lower than that of the alternative model, all the calculated temperatures from the default model decrease more slowly than those from the alternative model, and the calculated heat flux from the default model is always lower than that from the alternative model in the upper part of the condensing tube, and they are similar in the lower part.

4. Simulation results of base case calculations show that the default model of RELAP5/MOD3.2 predicts well the experimental heat transfer coefficient with high inlet mixture flow rate and low inlet air mass fraction, but it always under-predicts the experimental data except for the inlet condition. It is also known that the alternative model of RELAP5/MOD3.2 over-predicts the experimental data throughout the condensing tube, but it predicts well the experimental data with high inlet mixture flow rate except for the middle part of the condensing tube. From base case calculations it is considered to be that the effect of the inlet steam-air mixture flow rate is not properly considered in the default model, and the effect of the inlet air mass fraction in the alternative model.

5. The change of the divided node number in heat structure has little influence on the simulation results of the condensation phenomena with RELAP5/MOD3.2 both for the default and for the alternative model.

6. The simulation results for the sensitivity study show that the effects of the inlet steam-air mixture flow rate, the inlet air mass fraction, and the inlet saturated steam tempera-

ture are most influential in condensation experiments in the presence of noncondensable gas in a vertical tube. However, the effects of the coolant flow rate, the inlet coolant temperature, and the vented mixture temperature are less influential.

7. Run statistics show that the grind time of the default model is always higher than that of the alternative model and it is a little increased for both models when more volumes are included in RELAP5/MOD3.2 simulation. The required CPU time is the highest when the inlet mixture flow rate is the highest and both the inlet air mass fraction and the inlet saturated steam temperature are the lowest.

8. As both the default model and the alternative model can not predict well the experimental data, it is needed to develop a new correlation based on the experimental data produced over various operating ranges, and it can be applied as a new condensation model to simulate the condensation heat transfer of the steam-noncondensable gas mixture.

Bibliography

[1] S. H. Chang et al. "Korea Looks Beyond the Next Generation". *Nuclear Engineering International*, pages 12–16, Feb 1997.

[2] H. C. NO, S. I. Lee, H. S. Park, S. J. Kim, and H. T. Kim. "Validation Experiments and Code Development for Passive Safety Systems of CP-1300". In *Proc. of the 2nd Japan-Korea Seminar on Advanced Reactors*, pages 77–85, 1996.

[3] Sang Il Lee and Hee Cheon NO. "Assessment of RELAP5/MOD3.1 for Direct-Contact Condensation in the Core Makeup Tank of the CARR Passive Reactor". *Annals of Nuclear Energy*, 24(7):553–562, 1997.

[4] Hyoung Tae Kim and Hee Cheon NO. "Modification of Condensation Heat Transfer Model of RELAP5/MOD3.1 for the Simulation of Secondary Condensers". *Nuclear Technology*, 119:98–104, 1997.

[5] S.W. Lee, W.P. Baek and S. H. Chang. "Assessment of Passive Containment Cooling Concepts for Advanced Pressurized Water Reactors". *Annals of Nuclear Energy*, 24(6):467–475, 1997.

[6] B. S. Rao et al. "Simplified Boiling Water Reactor Design". In *1st JSME-ASME Int. Conf. on Nuclear Eng.(ICONE-1)*, pages 295–300, 1991.

[7] B. S. Shiralkar et al. "Thermal Hydraulic Aspects of the SBWR Design". *Int. Conf. on Design and Safety of Advanced NPPs*, 3:31.1.1–31.1.7, 1992.

[8] H. A. Upton et al. "Simplified Boiling Water Reactor Passive Safety Features". In *2st ASME-JSME Int. Conf. on Nuclear Eng.(ICONE-2)*, volume 1, pages 705–712, 1993.

[9] K. M. Vierow. *"Behavior of Steam-Air Systems Condensing in Concurrent Vertical Downflow"*. Ms thesis, U.C.B., 1990.

[10] K. M. Vierow and V. E. Schrock. "Condensation in a Natural Circulation Loop with Noncondensable Gases: Part I - Heat Transfer". In *Proc. of the Int. Conf. on Multiphase Flows '91*, pages 183–186, 1991.

[11] D. G. Ogg. *"Vertical Downflow Condensation Heat Transfer in Gas-Steam Mixtures"*. Ms thesis, U.C.B., 1991.

[12] M. Siddique, M. W. Golay and M. S. Kazimi. "Local Heat Transfer Coefficients for Forced-Convection of Steam in a Vertical Tube in the Presence of a Noncondensable Gas". *Nuclear technology*, 102:386–402, 1993.

[13] M. Siddique, M. W. Golay and M. S. Kazimi. "Theoretical Modeling of Forced Convection Condensation of Steam in a Vertical Tube in the Presence of a Noncondensable Gas". *Nuclear technology*, 106:202–214, 1994.

[14] H. A. Hasanein, M. W. Golay and M. S. Kazimi. *"Steam Condensation in the Presence of Noncondensable Gases under Forced Convection Conditions"*. M.I.T., MIT-ANP-TR-024, 1994.

[15] H. Araki, Y. Kataoka and M. Murase. "Measurement of Condensation Heat Transfer Coefficient Inside a Vertical Tube in the Presence of Noncondensable Gas". *Journal of nuclear science and technology*, 32(6):517–526, 1995.

[16] S. Z. Kuhn. *"Investigation of Heat Transfer from Condensing Steam-Gas Mixtures and Turbulent Films Flowing Downward Inside a Vertical Tube"*. Phd thesis, M.I.T., 1995.

[17] W.S. Yeung, J. Shirkov and F. Seifaee. "RELAP5/MOD3 Modeling of Water Column Rejoining and a Water Slug Propelled by Noncondensable Gas". *Nuclear Technology*, 108:387–394, 1994.

[18] Ki Yong CHOI, Hyun Sik PARK, Sang Jae KIM, Hee Cheon NO and Yong Seok BANG. "Assessment and Improvement of Condensation Models in RELAP5/MOD3.2". *submitted to the Nuclear Technology*, 1997.

[19] V. H. Ransom et al. "RELAP5/MOD3 Code Manual". NUREG/CR-5535, INEL, June 1995.

[20] W. Nusselt. "Die Oberflachenkondensation des Wasserdampfes". *Z. Ver. Deutsch. Ing.*, 1916.

[21] M. M. Shah. "A General Correlation for Heat Transfer during Film Condensation Inside Pipes". *Int.J. Heat Mass Transfer*, 22:547–556, 1979.

[22] A. P. Colburn and O. A. Hougen. "Design of Cooler Condensers for Mixtures of Vapors with Non-condensing Gases". *Industrial and Engineering Chemistry*, 26(11):1178–1182, 1934.

[23] J. C. Chato. "Laminar Condensation inside Horizontal and Inclined Tubes". *American Society of Heating, Refrigeration and Air Conditioning Engineering Journal*, 4:52–60, 1962.

[24] W. M. Rohsenow and Y. H. Choi. *"Heat Mass and Momentum Transfer"*. Prentice Hall, New Jersey, 1961.

[25] W. M. Kays and E. Y. Leung. "Heat transfer in annular passages-hydrodynamically developed turbulent flow with arbitrarily prescribed heat flux". *Int.J.Heat Mass Transfer*, 6:537–557, 1963.

[26] W. M. Kays and M. E. Crawford. *"Convective Heat and Mass Transfer"*. McGraw-Hill, Inc., 1993.

Appendix A

Test facility and its instrumentation

The experimental facility consists of a steam tank including a $100kW$ heater, a steam-noncondensable gas mixture supply line, a test section with a condensing tube and its surrounding coolant jacket, a lower plenum, venting and draining systems, and a unit of data acquisition system. The schematic diagram of the experimental apparatus is shown in Figure 2.1.

Steam and noncondensable gas supply

The steam tank functions as a containment. It is a cylindrical stainless steel pipe, which is $1540mm$ in height, $1000mm$ in inner diameter and $10mm$ in thickness on the top and bottom of which 12-mm-thick stainless steel caps are welded. The total height is $2000mm$ and the total volume is $1.332m^3$. It has a heater, two level gauges, a manhole, two sight glass and a relief valve.

The $108kW$ heater is a highly insulated, sheathed and flanged immersion heater which is located in the lower part of the steam tank in a horizontal direction. 36 heaters whose capacities are $3kW$ each are connected in δ-parallel. It is finely controlled by a $350A$ SCR power controller with a high precision voltmeter, an ampere-meter, and a watt-meter, which can be controlled automatically or manually.

A water refill line is attached to the upper demineralized water reservoir and during refilling the demineralized water is supplied from the reservoir by gravity. The two level gauges is installed to indicate the initial water level.

Steam is generated from the steam tank and is mixed with the supplied noncondensable gas in the steam tank. The noncondensable gas is supplied by the noncondensable gas supply line, and the vacuum can be achieved using a vacuum pump. Steam-noncondensable gas mixture gives a predetermined pressure in the steam tank to give an initial condition in thermal equilibrium and in homogeneous state. The noncondensable gas is injected into the steam tank continuously to give a continuous initial steam-noncondensable gas mass fraction, or to keep a total air inventory.

Even though the pressure of the steam tank is a little changed due to the injection of the noncondensable gas and the ejecting of the steam-noncondensable mixture, the steam tank will be in quasi-steady state because the noncondensable gas is injected deliberately to preserve the pressure, the temperature and the initial mass fraction of the noncondensable gas.

Test section

The steam-noncondensable gas mixture is supplied through a 1 inch pipe with a vortex flow meter. The mixture is made to keep uniform velocity distribution and its temperature and pressure are measured in the inlet of the test section. The upper plenum is a 2 inch pipe with tabs to install a thermocouple and a pressure transducer.

The test section consists of an inner condensing tube and an outer coolant jacket. The inner tube of the heat exchanger is a stainless steel pipe of $50.8mm$ in outer diameter, $1.65mm$ in thickness, and $2400mm$ in length. At 12 different axial locations each J-type thermocouple is welded on the outer surface of the condensing tube to measure the outer surface temperatures, welded through the condensing tube to measure the mixture bulk temperatures, and installed on the outer side of the coolant jacket to measure the coolant temperatures. These three kind of temperature sensors are located irregularly so that the

distance between each temperature measuring probes are chosen to be the same total heat transfer in each interval. They are located at 0, 10, 22, 36.5, 53.5, 73, 95, 119.5, 146, 175, 206.5, 240cm from the inlet of the uninsulated test section. The thermocouples are located densely at the inlet of the steam-noncondensable gas mixture because the heat transfer is high and most important in that region.

The inner tube is surrounded with a concentric coolant jacket pipe which is 100mm in inner diameter and 10mm in thickness, and the concentric jacket can be divided with three parts with the total length of 2400m. There are another two small jackets at the inlet and outlet of the coolant jacket. They are installed to stabilize the flow inside the coolant jacket. The lower one is designed to minimize the effects of the developing region at the inlet of the jacket and the upper one is designed to minimize the multi-dimensional effects at the outlet of the jacket.

The cooling water flows upward through the annulus and the steam-noncondensable gas mixture flows downward. The cooling water is supplied to the lower end of the jacket pipe in an once-through mode by a calibrated rotameter and a flow control valve, and is dumped to the drain after its temperature is increased. Two rotameters are used to measure the coolant flow rates. The coolant flow in the cooling jacket is in a turbulent regime because Reynolds number is about 2800 for the minimum flow rate of 363kg/hr.

Lower plenum

The lower plenum is a small hexahedral tank with the dimension of 200mm and 200mm in the bottom plate and 150mm in height. It is located at the outlet of the test section to help measure the temperature with a J-type thermocouple, and the pressure with a pressure transmitter. The level gauge is also used to check the level of the condensate in the lower plenum. It is connected to drain lines, a venting line and the outlet of the test section.

Venting and drain systems

The steam-noncondensable gas mixture is vented through the venting line and the condensate liquid from the outlet of the test section is drained down to the drain tank separately. The drain tank is connected to the lower plenum with the drain line and the pressure balancing line. The condensate liquid is drained to the drain tank through the drain line, and the pressure balancing line is used to equalize the pressure between the drain tank and the lower plenum. The valve on the vent line is regulated to keep the system pressure constant, and to change the venting rate. The vented mixture flow rate is measured.

Instrumentation and data acquisition system

Table 2.2 summarizes the instrumentation of PCCS experimental apparatus. All the signals from detectors are current output or voltage output including the output from the thermocouple. $4 \sim 20mA$ current signals from the pressure transducer and the vortex flow meter are converted to $1 \sim 5V$ voltage signals using an multi-channel current-to-voltage converter. The temperature signals are compensated to give accurate temperature data. All signals are applied to the Hewlett Packard 44708H high voltage relay multiplexer to give a reliable temperature and voltage data. Sampled experimental data is acquired using the HP3852A control unit and the data is transferred to IBM-PC/AT using the RS232C interface.

Appendix B

Data reduction method

Calculation of coolant bulk mean temperature

Kuhn[16] calculated the coolant bulk temperature in an annulus by measuring temperatures at the inner and the outer walls of the annulus, and using the numerically calculated temperature shape factors. The shape factors, F, are calculated for various inner and outer wall temperatures and coolant flow rates by solving the turbulent $k-\epsilon$ equations.

A simplified method to calculate the mean bulk coolant temperature is developed, which is a modified form of Kays[25]. It uses the empirical velocity profile and eddy diffusivity profile without solving the turbulent $k-\epsilon$ equations.

If the heat transfer in annular passages is considered for the hydrodynamically developed turbulent flow with arbitrarily prescribed heat flux, the energy differential equation can be written as follows:

$$\frac{\partial}{\partial r}\left[r(\alpha+\epsilon_H)\frac{\partial T(r,x)}{\partial r}\right] = ru(r)\frac{\partial T(r,x)}{\partial x} \tag{B.1}$$

The radius at which the maximum axial velocity is observed can be expressed by the following relationships[25].

$$s^* = (r^*)^{0.343} \tag{B.2}$$

where r^* is the annulus radius ratio, r_i/r_o, and s^* is $(\overline{s}-r^*)/(1-\overline{s})$. $\overline{s}$ is the ratio of the

radius at the maximum axial velocity, s, to the outer radius of the annulus, r_o.

The flow area in annular passage is broken into four sections radially at a certain axial location: a sublayer near the inner surface(Region I); a sublayer near the outer surface(Region II); a fully turbulent region from the inner sublayer to the point of maximum velocity(Region III); and a fully turbulent region from the outer sublayer to the point of maximum velocity(Region IV). Their velocity profiles and eddy diffusivity profiles can be described respectively, as follows:

$$\textit{Region I} \quad : y_i^+ < 10.8, \quad u^+ = y_i^+ \tag{B.3}$$

$$\textit{Region II} \quad : y_i^+ > 10.8, \quad u^+ = a y_i^+ + b \tag{B.4}$$

$$\textit{Region III} \quad : y_o^+ > 10.8, \quad u^+ = 2.5 y_o^+ + 5.5 \tag{B.5}$$

$$\textit{Region IV} \quad : y_o^+ < 10.8, \quad u^+ = y_o^+ \tag{B.6}$$

where $y_o = r_o - r$, $y_i = r - r_i$, $u^+ = \overline{u}/u_\tau = \overline{u}/u_\infty/\sqrt{c_f/2}$, and $y^+ = y u_\tau/\mu$.

The velocity profile for the wall coordinate is used at Region I and Region IV, and the velocity profile of Nikuradse equation[26] for the tube coordinate is used at Region III. At region II the velocity profile for the tube is used and the unknown constants, a and b, are calculated using Kay's method. The momentum eddy diffusivity ϵ_M/μ is also calculated from Kay's method and the thermal eddy diffusivity is given from the calculated momentum eddy diffusivity as follows:

$$Pr_T = \frac{\mu_T c_p}{\lambda_T} = 0.9 \tag{B.7}$$

Since the velocity, the momentum and the thermal eddy diffusivity profiles are all known, the energy equation can be solved to give the radial temperature distribution and thus the local mean coolant temperature.

Local heat flux

Local heat flux is typically obtained in terms of the axial gradient of the measured coolant bulk temperature.

$$q'' = \frac{\dot{m}c_p}{\pi d} \cdot \frac{dT_{cool}}{dL} \tag{B.8}$$

The accuracy of the calculated heat flux mainly depends on the coolant bulk temperature distribution.

Another method available to obtain the local heat flux is to use the Fourier's conduction law.

$$q'' = \frac{k}{t_{wall}} \cdot (T_{w,in} - T_{w,out}) \tag{B.9}$$

To determine the heat transfer two temperature measuring devices are installed on either side of the material to be measured. The accuracy of the heat flux mainly depends on the wall temperature measurement device, but error can be generated during the positioning of the device. To measure reasonably accurate inner and outer wall temperatures, the original thickness of the isolation condenser must be increased.

As an effective method to measure the heat transfer through any surface material like the condensing tube, the heat flux sensor is developed by RdF corporation. The heat flux sensor measure the heat transfer through a surface by differentiating temperature between opposite sides of certain rigid materials thereby allowing a direct measurement of the heat transfer through the material surface with a known thermal resistance.

In these experiments the heat flux is calculated by the temperature gradient of the coolant bulk temperature and is cross-checked with the directly measured one with the RdF heat flux sensor at a specific location of the condensing tube.

Condensation heat transfer coefficient

To obtain local heat transfer coefficient experimentally, it is necessary to determine the local heat flux and the temperature difference between the steam-noncondensable gas mixture bulk

and the inner wall.

$$h = \frac{q''}{(T_{mix} - T_{w,in})} \tag{B.10}$$

, where T_{mix} is the steam-noncondensable gas mixture bulk temperature and $T_{w,in}$ is the inner wall temperature of the condensing tube.

The inner wall temperature of the condensing tube

The inner wall temperature of the condensing tube can be expressed using the measured outer wall temperature and the calculated heat flux, as follows:

$$T_{w,in}(x) = T_{w,out}(x) + q''(x) \cdot \frac{ln(D_{out}/D_{in})D_{hydraulic}}{\pi k_{ss304}} \tag{B.11}$$

where D_{in} is the inner wall diameter, D_{out} the outer wall diameter, $D_{hydraulic}$ the hydraulic diameter, and k_{ss304} the thermal conductivity of the condensing tube.

Appendix C
RELPA5/MOD3.2 Input Listing

C-1. Base case calculation with default model (Experiments : #12b)

```
=RELAP5/MOD3.2 Simulation
*
****************************************
*Condensation Experiment in the presence
*of noncondensible gas in a Vertical Tube
*Dec 9. 1997 by HSPARK
****************************************
*
***********************************
* miscellaneous control cards
***********************************
*
100 new transnt
101 run
*
105 10. 20.
110 air
*
***********************************
* time step cards
***********************************
*
* end min.st max ctrl minor major rstplt
201 10. 1.0e-8 0.025 3 100 400 400
202 100. 1.0e-8 0.05 3 500 2000 2000
203 1000. 1.0e-8 0.1 3 2500 10000 10000
204 5000. 1.0e-8 0.1 3 5000 20000 20000
*204 5000. 1.0e-8 0.1 3 5000 20000 20000
*201 10. 1.0e-8 0.00001 3 2000000 10000000 10000000
*
* original time step
*201 500. 1.0e-8 0.005 3 2000 10000 10000
*
*
***********************************
* trip logic
***********************************
*
*
502 time 0 lt null 0. 0. n 0.0
506 time 0 gt null 0. 0. n -1.0
508 quala 150010000 gt null 0. 0.8 n 0
*
*
****************************************
* hydrodynamic data :
* steam-air mixture tube
****************************************
*
*
* component 100 : S/G using time dependent volume
* name type
1000000 tdv100 tmdpvol
* area length vol x angle elev rough dhydr vflag
1000101 2.0 2.0 0.0 0.0 0.0 0.0 1.e-4 0.0 00000
* noncondensible gas(air)
* cntrl
1000200 004
* var pressure temp. eq.quality
1000201 0.0 0.46546675e6 0.4165528e3 1.0
*
* component 105 : steam flow initiation in kg/s
* name type
1050000 tdj105 tmdpjun
* from to area
* ccc000000 cccvv000n
1050101 100000000 115010001 0.00049
* cntrl trip
1050200 1 502
* var waterflow steamflow interface vel.
```

```
1050201 -1.0 0.0 0.009087 0.0
1050202 0 0.0 0.009087 0.0
*
* component 115 : pipe to upper plenum
* name type
1150000 sv115 snglvol
* area length vol x angle
1150101 0.00049 0.07 0.0 0.0 90.
* elev rough dh vflag
1150102 0.07 1.e-4 0.0 00000
* cntrl pressure quality
*1150200 002 0.46546675e6 1.0
* cntrl pressure temp.
1150200 003 0.46546675e6 0.35474181e3
*
*
* component 120 : upper plenum
* name type
1200000 b120 branch
* no. jun cntrl
1200001 2 1
* area=10cm length vol x angle elev rough dh vflag
1200101 0.007854 0.20 0.0 0. -90. -0.20 1.e-4 0.0 11000
* cntrl pressure quality
*1200200 002 0.46546675e6 1.0
* cntrl pressure temp.
1200200 003 0.46546675e6 0.35474181e3
* from to area kforw kbackw jflag
* cccn101 cccvv000n
1201101 115010002 120010002 0.000490 225.847 120.438
000000
1202101 120010002 140010001 0.001772 7.608 11.783
000000
* waterflow steamflow x
* cccn201
1201201 0.0 0.009087 0.0
1202201 0.0 0.009087 0.0
*
*
* component 140 : condensing tube
* name type
1400000 pipe140 pipe
* nv: no. vol
1400001 13
* area nv
1400101 0.001772 13
* length vn
* ccc0301 - ccc0399
1400301 0.500 1
1400302 0.100 2
1400303 0.120 3
1400304 0.145 4
1400305 0.170 5
1400306 0.195 6
1400307 0.220 7
1400308 0.245 8
1400309 0.265 9
1400310 0.290 10
1400311 0.315 11
1400312 0.335 12
1400313 0.400 13
* ccc0301 - ccc0399
*1400301 0.500 1
*1400302 0.200 12
*1400313 0.400 13
* volume nv
*1400401 0.0 13
* angle vn
1400601 -90.0 13
* rough dhydr no. vol
1400801 1.e-4 0.0 13
* vflag no. vol
1401001 00000 13
* jflag no. jun
1401101 000000 12
* cntrl pressure temp. nv
*ccc1201-ccc1299
1800200 003
1401201 003 0.46546675e6 0.35474181e3 0.0 0.0 0.0 1
1401202 003 0.46546675e6 0.35474181e3 0.0 0.0 0.0 2
1401203 003 0.46546675e6 0.35474181e3 0.0 0.0 0.0 3
1401204 003 0.46546675e6 0.35474181e3 0.0 0.0 0.0 4
1401205 003 0.46546675e6 0.35474181e3 0.0 0.0 0.0 5
1401206 003 0.46546675e6 0.35474181e3 0.0 0.0 0.0 6
1401207 003 0.46546675e6 0.35474181e3 0.0 0.0 0.0 7
1401208 003 0.46546675e6 0.35474181e3 0.0 0.0 0.0 8
1401209 003 0.46546675e6 0.35474181e3 0.0 0.0 0.0 9
1401210 003 0.46546675e6 0.35474181e3 0.0 0.0 0.0 10
1401211 003 0.46546675e6 0.35474181e3 0.0 0.0 0.0 11
1401212 003 0.46546675e6 0.35474181e3 0.0 0.0 0.0 12
1401213 003 0.46546675e6 0.35474181e3 0.0 0.0 0.0 13
* cntrl
```

```
1401300 1
* water flow steam flow int.vel jn
1401301 0.0 0.0 0.0 12
*
*
* component 145 : condensing tube to lower plenum
* name type
1450000 sj145 sngljun
* from to area kforw kbackw jflag
1450101 140130002 150010001 0.001772 11.783 7.608
0001000
* cntrl waterflow steamflow x
1450201 1 0.0 0.0 0.0
*
* component 150 : lower plenum
* name type
1500000 pipe150 pipe
* nv
1500001 3
* area nv
1500101 0.007854 3
* length vn
1500301 0.10 1
1500302 0.10 2
1500303 0.10 3
* volume nv
1500401 0.0 3
* angle nv
1500601 -90.0 3
* rough dhydr nv
1500801 1.e-4 0.0 3
* vflag nv
1501001 00000 3
* jflag nj
1501101 000000 2
* cntrl pressure temp. eq.quality vn
1501201 004 0.46546675e6 0.35474181e3 1.0 0.0 0.0 1
1501202 004 0.46546675e6 0.35474181e3 1.0 0.0 0.0 2
1501203 004 0.46546675e6 0.35474181e3 1.0 0.0 0.0 3
* cntrl
1501300 1
* waterflow steamflow int.vel nj
1501301 0.0 0.0 0.0 2
*
*
************************************
* hydrodynamic data : venting line
************************************
*
*
* component 155 : lower plenum to drain tank
* name type
1550000 sj155 sngljun
* from to areav kforw kbackw jflag
1550101 150030002 160050002 0.00001 923317.24
923317.24 0001000
* cntrl waterflow steamflow x
1550201 1 0.0 0.0 0.0
*
*
* component 156 : lower plenum to drain pipe
* name type
1560000 sj156 sngljun
* from to areav kforw kbackw jflag
1560101 150030002 157050002 0.00012 2109.13 4153.80
0001000
* cntrl waterflow steamflow x
1560201 1 0.0 0.0 0.0
*
* component 157 : drain pipe
* name type
1570000 pipe157 pipe
* nv
1570001 5
* area nv
1570101 0.00012 5
* length vn
1570301 0.20 5
* volume nv
1570401 0.0 5
* angle nv
1570601 90.0 5
* rough dhydr nv
1570801 1.e-4 0.0 5
* vflag nv
1571001 00000 5
* jflag nj
1571101 000000 4
* cntrl pressure temp. eq.quality vn
1571201 004 0.46546675e6 0.35474181e3 1.0 0.0 0.0 1
1571202 004 0.46546675e6 0.35474181e3 0.5 0.0 0.0 2
1571203 004 0.46546675e6 0.35474181e3 0.0 0.0 0.0 3
```

```
1571204 004 0.46546675e6 0.35474181e3 0.0 0.0 0.0 4
1571205 004 0.46546675e6 0.35474181e3 0.0 0.0 0.0 5
* cntrl
1571300 1
* waterflow steamflow int.vel nj
1571301 0.0 0.0 0.0 4
*
*
* component 158 : drain pipe to drain tank
* name type
1580000 sj158 sngljun
* from to areav kforw kbackw jflag
1580101 157010001 160010001 0.00012 42823936.0
21415240.0 0001000
* cntrl waterflow steamflow x
1580201 1 0.0 0.0 0.0
*
*
* component 160 : drain tank
* name type
1600000 pipe160 pipe
* nv
1600001 5
* area nv
1600101 0.7854 5
* length vn
1600301 0.20 5
* volume nv
1600401 0.0 5
* angle nv
1600601 90.0 5
* rough dhydr nv
1600801 1.e-4 0.0 5
* vflag nv
1601001 00000 5
* jflag nj
1601101 000000 4
* cntrl pressure temp. eq.quality vn
1601201 004 0.46546675e6 0.35474181e3 1.0 0.0 0.0 1
1601202 004 0.46546675e6 0.35474181e3 0.5 0.0 0.0 2
1601203 004 0.46546675e6 0.35474181e3 0.0 0.0 0.0 3
1601204 004 0.46546675e6 0.35474181e3 0.0 0.0 0.0 4
1601205 004 0.46546675e6 0.35474181e3 0.0 0.0 0.0 5
* cntrl
1601300 1
* waterflow steamflow int.vel nj
1601301 0.0 0.0 0.0 4
*
* componet 175 : valve for venting
* name type
1750000 vv175 valve
* from to areav kforw kback jflag
1750101 150030002 180000000 0.00012 2109.13 4153.80
000100
* cntrl waterflow steamflow interface velocity
1750201 1 0.0 0.0 0.0
* valve type
1750300 trpvlv
* trip number(open when true)
1750301 506
*
*
* component 180 : venting simulation using tdv
* name type
1800000 tdv181 tmdpvol
* area length vol x angle elev rough dhydr vflag
1800101 2.0 2.0 0.0 0.0 0.0 0.0 0.0 0.0 00000
* cntrl
1800200 003
* var pressure temp.
1800201 0.0 0.46546675e6 0.35474181e3
*
*
****************************************
* hydrodynamic data : coolant water annulus
****************************************
*
*
* component 200 : coolant source simulation using tdv
* name type
2000000 tdv200 tmdpvol
* area length vol x angle elev rough dhydr vflag
2000101 2.0 2.0 0.0 0.0 0.0 0.0 0.0 0.0 00000
* cntrl
2000200 003
* var p(1atm) temp.
2000201 0.0 0.1013e6 0.3024605e3
*
* component 210 : coolant water flow initiation -> 0.13kg/s
* component 210 *
* name type
2100000 tdj210 tmdpjun
```

```
* from to area
2100101 200000000 240010001 0.00049
* cntrl trip
2100200 1 502
* var waterflow steamflow x
2100201 -1.0 0.1514 0.0 0.0
2100202 0. 0.1514 0.0 0.0
*
* component 240 : outer tube for coolant water
* name type
2400000 out_tube annulus
* nv
2400001 11
* area nv
2400101 0.005151 11
* length vn
*2400301 0.200 11
2400301 0.335 1
2400302 0.315 2
2400303 0.290 3
2400304 0.265 4
2400305 0.245 5
2400306 0.220 6
2400307 0.195 7
2400308 0.170 8
2400309 0.145 9
2400310 0.120 10
2400311 0.100 11
* volume nv
2400401 0.0 11
* angle nv
2400601 90.0 11
* rough hd nv
2400801 1.e-4 0.0 11
* vflag nv
2401001 00010 11
* jflag nj
2401101 000020 10
* cntrl pressure temp. vn
2401201 003 0.1013e6 0.3024605e3 0.0 0.0 0.0 1
2401202 003 0.1013e6 0.3024605e3 0.0 0.0 0.0 2
2401203 003 0.1013e6 0.3024605e3 0.0 0.0 0.0 3
2401204 003 0.1013e6 0.3024605e3 0.0 0.0 0.0 4
2401205 003 0.1013e6 0.3024605e3 0.0 0.0 0.0 5
2401206 003 0.1013e6 0.3024605e3 0.0 0.0 0.0 6
2401207 003 0.1013e6 0.3024605e3 0.0 0.0 0.0 7
2401208 003 0.1013e6 0.3024605e3 0.0 0.0 0.0 8
2401209 003 0.1013e6 0.3024605e3 0.0 0.0 0.0 9
2401210 003 0.1013e6 0.3024605e3 0.0 0.0 0.0 10
2401211 003 0.1013e6 0.3024605e3 0.0 0.0 0.0 11
* cntrl
2401300 1
* waterflow steamflow int.vel nj
2401301 0.1514 0.0 0.0 10
*
* component 270 : outer tube to coolant outlet
* name type
2700000 sj270 sngljun
* from to area kforw kbackw jflag
2700101  240110002  280000000  0.00049  50.0  90.48
0001000
* cntrl waterflow steamflow x
2700201 1 0.1514 0.0 0.0
*
* component 280 : coolant water dumping
* name type
2800000 tdv280 tmdpvol
* area length vol x angle elev rough dhydr vflag
2800101 2.0 2.0 0.0 0.0 0.0 0.0 0.0 0.0 00000
* cntrl
2800200 003
* var p(1atm) temp.
2800201 0.0 0.1013e6 0.3024605e3
*
*
****************************************
* heat structure input : pipe140 <-> annulus240
* (condensing tube simulation)
****************************************
*
*
* heat structure 140 : heat transfer simulation through pipe
11400000 11 4 2 1 0.02375
11400100 0 1
11400101 3 0.02540
11400201 5 3
11400301 0 3
11400401 373.0 4
*
*11400501 140020000 0 101 1 0.200 1
*11400502 140030000 10000 101 1 0.200 11
*
```

```
*11400601 240110000 0 101 1 0.200 1
*11400602 240100000 -10000 101 1 0.200 11
*
*
11400501 140020000 0 101 1 0.100 1
11400502 140030000 0 101 1 0.120 2
11400503 140040000 0 101 1 0.145 3
11400504 140050000 0 101 1 0.170 4
11400505 140060000 0 101 1 0.195 5
11400506 140070000 0 101 1 0.220 6
11400507 140080000 0 101 1 0.245 7
11400508 140090000 0 101 1 0.265 8
11400509 140100000 0 101 1 0.290 9
11400510 140110000 0 101 1 0.315 10
11400511 140120000 0 101 1 0.335 11
*
11400601 240110000 0 101 1 0.100 1
11400602 240100000 0 101 1 0.120 2
11400603 240090000 0 101 1 0.145 3
11400604 240080000 0 101 1 0.170 4
11400605 240070000 0 101 1 0.195 5
11400606 240060000 0 101 1 0.220 6
11400607 240050000 0 101 1 0.245 7
11400608 240040000 0 101 1 0.265 8
11400609 240030000 0 101 1 0.290 9
11400610 240020000 0 101 1 0.315 10
11400611 240010000 0 101 1 0.335 11
*
11400701 0 0.0 0.0 0.0 11
11400801 0 10.0 10.0 10.0 10.0 0 0 1.0 11
11400901 0 10.0 10.0 10.0 10.0 0 0 1.0 11
*
****************************************
```

```
* heat structure thermal property data : SUS (005) 18cr-8ni
****************************************
*
20100500 tbl/fctn 1 1
*
* temp(k) thermal conductivity(w/m.k)
20100501 0.2732611e+03 0.1489124e+02
20100502 0.2942611e+03 0.1489124e+02
20100503 0.3109278e+03 0.1505739e+02
20100504 0.3664834e+03 0.1609584e+02
20100505 0.4220389e+03 0.1696813e+02
20100506 0.4775945e+03 0.1800657e+02
20100507 0.5331500e+03 0.1885809e+02
20100508 0.5887056e+03 0.1956423e+02
20100509 0.6442611e+03 0.2041575e+02
20100510 0.8109278e+03 0.2297030e+02
20100511 0.9220389e+03 0.2423029e+02
20100512 1.9220389e+03 0.2423029e+02
*
* temp(k) volumetric heat capacity(j/m3.k)
20100551 0.2742611e+03 0.3831330e+07
20100552 0.3109278e+03 0.3831330e+07
20100553 0.3664834e+03 0.3985580e+07
20100554 0.4220389e+03 0.4105300e+07
20100555 0.4775945e+03 0.4224090e+07
20100556 0.5331500e+03 0.4308800e+07
20100557 0.5887056e+03 0.4359790e+07
20100558 0.6442611e+03 0.4410320e+07
20100559 0.8109278e+03 0.4561910e+07
20100560 0.9220389e+03 0.4625250e+07
20100561 1.9220389e+03 0.4625250e+07
*
. end of file
```

C-2. Base case calculation with alternative model (Experiments : #12b)

Modification of C-1

1. heat structure input

```
**************************************
* heat structure input : pipe140 <-> annulus240
* (condensing tube simulation)
**************************************
* heat structure 140 : heat transfer simulation through pipe
11400000 11 4 2 1 0.02375
11400100 0 1
11400101 3 0.02540
11400201 5 3
11400301 0 3
11400401 373.0 4
*
*11400501 140020000 0 153 1 0.200 1
*11400502 140030000 10000 153 1 0.200 11
*
*11400601 240110000 0 153 1 0.200 1
*11400602 240100000 -10000 153 1 0.200 11
*
11400501 140020000 0 153 1 0.100 1
11400502 140030000 0 153 1 0.120 2
11400503 140040000 0 153 1 0.145 3
11400504 140050000 0 153 1 0.170 4
11400505 140060000 0 153 1 0.195 5
11400506 140070000 0 153 1 0.220 6
11400507 140080000 0 153 1 0.245 7
11400508 140090000 0 153 1 0.265 8
11400509 140100000 0 153 1 0.290 9
11400510 140110000 0 153 1 0.315 10
11400511 140120000 0 153 1 0.335 11
*
11400601 240110000 0 153 1 0.100 1
11400602 240100000 0 153 1 0.120 2
11400603 240090000 0 153 1 0.145 3
11400604 240080000 0 153 1 0.170 4
11400605 240070000 0 153 1 0.195 5
11400606 240060000 0 153 1 0.220 6
11400607 240050000 0 153 1 0.245 7
11400608 240040000 0 153 1 0.265 8
11400609 240030000 0 153 1 0.290 9
11400610 240020000 0 153 1 0.315 10
11400611 240010000 0 153 1 0.335 11
*
11400701 0 0.0 0.0 0.0 11
11400801 0 10.0 10.0 10.0 10.0 0 0 1.0 11
11400901 0 10.0 10.0 10.0 10.0 0 0 1.0 11
*
```

C-3. Simulation for sensitivity study with default model (Simulation : #ss0)

Modification of C-1

1. time step

```
=RELAP5/MOD3.2 Simulation
*
****************************************
*Condensation Experiment in the presence
*of noncondensible gas in a Vertical Tube
*Dec 9. 1997 by HSPARK
****************************************
*
*
************************************
* miscellaneous control cards
************************************
*
*
100 new transnt
101 run
*
105 10. 20.
110 air
*
*
************************************
* time step cards
************************************
*
*
* end min.st max ctrl minor major rstplt
201 10. 1.0e-8 0.025 3 100 400 400
202 100. 1.0e-8 0.05 3 500 2000 2000
203 250. 1.0e-8 0.1 3 2500 10000 10000
*204 5000. 1.0e-8 0.1 3 5000 20000 20000
*201 10. 1.0e-8 0.00001 3 2000000 10000000 10000000
*
* original time step
*201 500. 1.0e-8 0.005 3 2000 10000 10000
*
*
************************************
* trip logic
************************************
*
*
502 time 0 lt null 0. 0. n 0.0
506 time 0 gt null 0. 0. n -1.0
508 quala 150010000 gt null 0. 0.8 n 0
*
*
****************************************
* hydrodynamic data : steam-air mixture tube
****************************************
*
*
* component 100 : S/G using time dependent volume
* name type
1000000 tdv100 tmdpvol
* area length vol x angle elev rough dhydr vflag
1000101 2.0 2.0 0.0 0.0 0.0 0.0 1.e-4 0.0 00000
* noncondensible gas(air)
* cntrl
1000200 004
* var pressure temp. eq.quality
1000201 0.0 0.46546675e6 0.4165528e3 1.0
*
*
* component 105 : steam flow initiation in kg/s
* name type
1050000 tdj105 tmdpjun
* from to area
* ccc000000 cccvv000n
1050101 100000000 115010001 0.00049
* cntrl trip
1050200 1 502
* var waterflow steamflow interface vel.
1050201 -1.0 0.0 0.009087 0.0
```

```
1050202 0 0.0 0.009087 0.0
*
*
* component 115 : pipe to upper plenum
* name type
1150000 sv115 snglvol
* area length vol x angle
1150101 0.00049 0.07 0.0 0.0 90.
* elev rough dh vflag
1150102 0.07 1.e-4 0.0 00000
* cntrl pressure quality
*1150200 002 0.46546675e6 1.0
* cntrl pressure temp.
1150200 003 0.46546675e6 0.35474181e3
*
*
* component 120 : upper plenum
* name type
1200000 b120 branch
* no. jun cntrl
1200001 2 1
* area=10cm length vol x angle elev rough dh vflag
1200101 0.007854 0.20 0.0 0. -90. -0.20 1.e-4 0.0 11000
* cntrl pressure quality
*1200200 002 0.46546675e6 1.0
* cntrl pressure temp.
1200200 003 0.46546675e6 0.35474181e3
* from to area kforw kbackw jflag
* cccn101 cccvv000n
1201101 115010002 120010002 0.000490 225.847 120.438
000000
1202101 120010002 140010001 0.001772 7.608 11.783
000000
* waterflow steamflow x
* cccn201
1201201 0.0 0.009087 0.0
1202201 0.0 0.009087 0.0
*
*
* component 140 : condensing tube
* name type
1400000 pipe140 pipe
* nv: no. vol
1400001 13
* area nv
1400101 0.001772 13
* length vn
* ccc0301 - ccc0399
1400301 0.500 1
1400302 0.100 2
1400303 0.120 3
1400304 0.145 4
1400305 0.170 5
1400306 0.195 6
1400307 0.220 7
1400308 0.245 8
1400309 0.265 9
1400310 0.290 10
1400311 0.315 11
1400312 0.335 12
1400313 0.400 13
* ccc0301 - ccc0399
*1400301 0.500 1
*1400302 0.200 12
*1400313 0.400 13
* volume nv
*1400401 0.0 13
* angle vn
1400601 -90.0 13
* rough dhydr no. vol
1400801 1.e-4 0.0 13
* vflag no. vol
1401001 00000 13
* jflag no. jun
1401101 000000 12
* cntrl pressure temp. nv
*ccc1201-ccc1299
1800200 003
1401201 003 0.46546675e6 0.35474181e3 0.0 0.0 0.0 1
1401202 003 0.46546675e6 0.35474181e3 0.0 0.0 0.0 2
1401203 003 0.46546675e6 0.35474181e3 0.0 0.0 0.0 3
1401204 003 0.46546675e6 0.35474181e3 0.0 0.0 0.0 4
1401205 003 0.46546675e6 0.35474181e3 0.0 0.0 0.0 5
1401206 003 0.46546675e6 0.35474181e3 0.0 0.0 0.0 6
1401207 003 0.46546675e6 0.35474181e3 0.0 0.0 0.0 7
1401208 003 0.46546675e6 0.35474181e3 0.0 0.0 0.0 8
1401209 003 0.46546675e6 0.35474181e3 0.0 0.0 0.0 9
1401210 003 0.46546675e6 0.35474181e3 0.0 0.0 0.0 10
1401211 003 0.46546675e6 0.35474181e3 0.0 0.0 0.0 11
1401212 003 0.46546675e6 0.35474181e3 0.0 0.0 0.0 12
1401213 003 0.46546675e6 0.35474181e3 0.0 0.0 0.0 13
* cntrl
```

```
1401300 1
* water flow steam flow int.vel jn
1401301 0.0 0.0 0.0 12
*
*
* component 145 : condensing tube to lower plenum
* name type
1450000 sj145 sngljun
* from to area kforw kbackw jflag
1450101 140130002 150010001 0.001772 11.783 7.608
0001000
* cntrl waterflow steamflow x
1450201 1 0.0 0.0 0.0
*
*
* component 150 : lower plenum
* name type
1500000 pipe150 pipe
* nv
1500001 3
* area nv
1500101 0.007854 3
* length vn
1500301 0.10 1
1500302 0.10 2
1500303 0.10 3
* volume nv
1500401 0.0 3
* angle nv
1500601 -90.0 3
* rough dhydr nv
1500801 1.e-4 0.0 3
* vflag nv
1501001 00000 3
* jflag nj
1501101 000000 2
* cntrl pressure temp. eq.quality vn
1501201 004 0.46546675e6 0.35474181e3 1.0 0.0 0.0 1
1501202 004 0.46546675e6 0.35474181e3 1.0 0.0 0.0 2
1501203 004 0.46546675e6 0.35474181e3 1.0 0.0 0.0 3
* cntrl
1501300 1
* waterflow steamflow int.vel nj
1501301 0.0 0.0 0.0 2
*
*
************************************
* hydrodynamic data : venting line
************************************
*
*
* component 155 : lower plenum to drain tank
* name type
1550000 sj155 sngljun
* from to areav kforw kbackw jflag
1550101 150030002 160050002 0.00001 923317.24
923317.24 0001000
* cntrl waterflow steamflow x
1550201 1 0.0 0.0 0.0
*
*
* component 156 : lower plenum to drain pipe
* name type
1560000 sj156 sngljun
* from to areav kforw kbackw jflag
1560101 150030002 157050002 0.00012 2109.13 4153.80
0001000
* cntrl waterflow steamflow x
1560201 1 0.0 0.0 0.0
*
*
* component 157 : drain pipe
* name type
1570000 pipe157 pipe
* nv
1570001 5
* area nv
1570101 0.00012 5
* length vn
1570301 0.20 5
* volume nv
1570401 0.0 5
* angle nv
1570601 90.0 5
* rough dhydr nv
1570801 1.e-4 0.0 5
* vflag nv
1571001 00000 5
* jflag nj
1571101 000000 4
* cntrl pressure temp. eq.quality vn
1571201 004 0.46546675e6 0.35474181e3 1.0 0.0 0.0 1
```

```
1571202 004 0.46546675e6 0.35474181e3 0.5 0.0 0.0 2
1571203 004 0.46546675e6 0.35474181e3 0.0 0.0 0.0 3
1571204 004 0.46546675e6 0.35474181e3 0.0 0.0 0.0 4
1571205 004 0.46546675e6 0.35474181e3 0.0 0.0 0.0 5
* cntrl
1571300 1
* waterflow steamflow int.vel nj
1571301 0.0 0.0 0.0 4
*
*
* component 158 : drain pipe to drain tank
* name type
1580000 sj158 sngljun
* from to areav kforw kbackw jflag
1580101  157010001  160010001  0.00012  42823936.0
21415240.0 0001000
* cntrl waterflow steamflow x
1580201 1 0.0 0.0 0.0
*
*
* component 160 : drain tank
* name type
1600000 pipe160 pipe
* nv
1600001 5
* area nv
1600101 0.7854 5
* length vn
1600301 0.20 5
* volume nv
1600401 0.0 5
* angle nv
1600601 90.0 5
* rough dhydr nv
1600801 1.e-4 0.0 5
* vflag nv
1601001 00000 5
* jflag nj
1601101 000000 4
* cntrl pressure temp. eq.quality vn
1601201 004 0.46546675e6 0.35474181e3 1.0 0.0 0.0 1
1601202 004 0.46546675e6 0.35474181e3 0.5 0.0 0.0 2
1601203 004 0.46546675e6 0.35474181e3 0.0 0.0 0.0 3
1601204 004 0.46546675e6 0.35474181e3 0.0 0.0 0.0 4
1601205 004 0.46546675e6 0.35474181e3 0.0 0.0 0.0 5
* cntrl
1601300 1
* waterflow steamflow int.vel nj
1601301 0.0 0.0 0.0 4
*
*
* componet 175 : valve for venting
* name type
1750000 vv175 valve
* from to areav kforw kback jflag
1750101 150030002 180000000 0.00012 2109.13 4153.80
000100
* cntrl waterflow steamflow interface velocity
1750201 1 0.0 0.0 0.0
* valve type
1750300 trpvlv
* trip number(open when true)
1750301 506
*
*
* component 180 : venting simulation using tdv
* name type
1800000 tdv181 tmdpvol
* area length vol x angle elev rough dhydr vflag
1800101 2.0 2.0 0.0 0.0 0.0 0.0 0.0 0.0 00000
* cntrl
1800200 003
* var pressure temp.
1800201 0.0 0.46546675e6 0.35474181e3
*
*
**************************************
* hydrodynamic data : coolant water annulus
**************************************
*
*
* component 200 : coolant source simulation using tdv
* name type
2000000 tdv200 tmdpvol
* area length vol x angle elev rough dhydr vflag
2000101 2.0 2.0 0.0 0.0 0.0 0.0 0.0 0.0 00000
* cntrl
2000200 003
* var p(1atm) temp.
2000201 0.0 0.1013e6 0.3024605e3
*
*
```

```
* component 210 : coolant water flow initiation -> 0.13kg/s
* component 210 *
* name type
2100000 tdj210 tmdpjun
* from to area
2100101 200000000 240010001 0.00049
* cntrl trip
2100200 1 502
* var waterflow steamflow x
2100201 -1.0 0.1514 0.0 0.0
2100202 0. 0.1514 0.0 0.0
*
*
* component 240 : outer tube for coolant water
* name type
2400000 out_tube annulus
* nv
2400001 11
* area nv
2400101 0.005151 11
* length vn
*2400301 0.200 11
2400301 0.335 1
2400302 0.315 2
2400303 0.290 3
2400304 0.265 4
2400305 0.245 5
2400306 0.220 6
2400307 0.195 7
2400308 0.170 8
2400309 0.145 9
2400310 0.120 10
2400311 0.100 11
* volume nv
2400401 0.0 11
* angle nv
2400601 90.0 11
* rough hd nv
2400801 1.e-4 0.0 11
* vflag nv
2401001 00010 11
* jflag nj
2401101 000020 10
* cntrl pressure temp. vn
2401201 003 0.1013e6 0.3024605e3 0.0 0.0 0.0 1
2401202 003 0.1013e6 0.3024605e3 0.0 0.0 0.0 2
2401203 003 0.1013e6 0.3024605e3 0.0 0.0 0.0 3
2401204 003 0.1013e6 0.3024605e3 0.0 0.0 0.0 4
2401205 003 0.1013e6 0.3024605e3 0.0 0.0 0.0 5
2401206 003 0.1013e6 0.3024605e3 0.0 0.0 0.0 6
2401207 003 0.1013e6 0.3024605e3 0.0 0.0 0.0 7
2401208 003 0.1013e6 0.3024605e3 0.0 0.0 0.0 8
2401209 003 0.1013e6 0.3024605e3 0.0 0.0 0.0 9
2401210 003 0.1013e6 0.3024605e3 0.0 0.0 0.0 10
2401211 003 0.1013e6 0.3024605e3 0.0 0.0 0.0 11
* cntrl
2401300 1
* waterflow steamflow int.vel nj
2401301 0.1514 0.0 0.0 10
*
*
* component 270 : outer tube to coolant outlet
* name type
2700000 sj270 sngljun
* from to area kforw kbackw jflag
2700101 240110002 280000000 0.00049 50.0 90.48
0001000
* cntrl waterflow steamflow x
2700201 1 0.1514 0.0 0.0
*
*
* component 280 : coolant water dumping
* name type
2800000 tdv280 tmdpvol
* area length vol x angle elev rough dhydr vflag
2800101 2.0 2.0 0.0 0.0 0.0 0.0 0.0 0.0 00000
* cntrl
2800200 003
* var p(1atm) temp.
2800201 0.0 0.1013e6 0.3024605e3
*
*
****************************************
* heat structure input : pipe140 <-> annulus240
* (condensing tube simulation)
****************************************
*
*
* heat structure 140 : heat transfer simulation through pipe
11400000 11 4 2 1 0.02375
11400100 0 1
11400101 3 0.02540
```

```
11400201 5 3
11400301 0 3
11400401 373.0 4
*
*11400501 140020000 0 101 1 0.200 1
*11400502 140030000 10000 101 1 0.200 11
*
*11400601 240110000 0 101 1 0.200 1
*11400602 240100000 -10000 101 1 0.200 11
*
*
11400501 140020000 0 101 1 0.100 1
11400502 140030000 0 101 1 0.120 2
11400503 140040000 0 101 1 0.145 3
11400504 140050000 0 101 1 0.170 4
11400505 140060000 0 101 1 0.195 5
11400506 140070000 0 101 1 0.220 6
11400507 140080000 0 101 1 0.245 7
11400508 140090000 0 101 1 0.265 8
11400509 140100000 0 101 1 0.290 9
11400510 140110000 0 101 1 0.315 10
11400511 140120000 0 101 1 0.335 11
*
11400601 240110000 0 101 1 0.100 1
11400602 240100000 0 101 1 0.120 2
11400603 240090000 0 101 1 0.145 3
11400604 240080000 0 101 1 0.170 4
11400605 240070000 0 101 1 0.195 5
11400606 240060000 0 101 1 0.220 6
11400607 240050000 0 101 1 0.245 7
11400608 240040000 0 101 1 0.265 8
11400609 240030000 0 101 1 0.290 9
11400610 240020000 0 101 1 0.315 10
11400611 240010000 0 101 1 0.335 11
*
11400701 0 0.0 0.0 0.0 11
11400801 0 10.0 10.0 10.0 10.0 0 0 1.0 11
11400901 0 10.0 10.0 10.0 10.0 0 0 1.0 11
*
*
****************************************
* heat structure thermal property data : SUS (005) 18cr-8ni
****************************************
*
*
20100500 tbl/fctn 1 1
*
* temp(k) thermal conductivity(w/m.k)
20100501 0.2732611e+03 0.1489124e+02
20100502 0.2942611e+03 0.1489124e+02
20100503 0.3109278e+03 0.1505739e+02
20100504 0.3664834e+03 0.1609584e+02
20100505 0.4220389e+03 0.1696813e+02
20100506 0.4775945e+03 0.1800657e+02
20100507 0.5331500e+03 0.1885809e+02
20100508 0.5887056e+03 0.1956423e+02
20100509 0.6442611e+03 0.2041575e+02
20100510 0.8109278e+03 0.2297030e+02
20100511 0.9220389e+03 0.2423029e+02
20100512 1.9220389e+03 0.2423029e+02
*
* temp(k) volumetric heat capacity(j/m3.k)
20100551 0.2742611e+03 0.3831330e+07
20100552 0.3109278e+03 0.3831330e+07
20100553 0.3664834e+03 0.3985580e+07
20100554 0.4220389e+03 0.4105300e+07
20100555 0.4775945e+03 0.4224090e+07
20100556 0.5331500e+03 0.4308800e+07
20100557 0.5887056e+03 0.4359790e+07
20100558 0.6442611e+03 0.4410320e+07
20100559 0.8109278e+03 0.4561910e+07
20100560 0.9220389e+03 0.4625250e+07
20100561 1.9220389e+03 0.4625250e+07
*
. end of file
```

C-4. Simulation for sensitivity study with alternative model (Simulation : #ss0)

Modification of C-3

1. heat structure input

```
**************************************
* heat structure input : pipe140 <-> annulus240
* (condensing tube simulation)
**************************************
*
*
* heat structure 140 : heat transfer simulation through pipe
11400000 11 4 2 1 0.02375
11400100 0 1
11400101 3 0.02540
11400201 5 3
11400301 0 3
11400401 373.0 4
*
*11400501 140020000 0 153 1 0.200 1
*11400502 140030000 10000 153 1 0.200 11
*
*11400601 240110000 0 153 1 0.200 1
*11400602 240100000 -10000 153 1 0.200 11
*
*
11400501 140020000 0 153 1 0.100 1
11400502 140030000 0 153 1 0.120 2
11400503 140040000 0 153 1 0.145 3
11400504 140050000 0 153 1 0.170 4
11400505 140060000 0 153 1 0.195 5
11400506 140070000 0 153 1 0.220 6
11400507 140080000 0 153 1 0.245 7
11400508 140090000 0 153 1 0.265 8
11400509 140100000 0 153 1 0.290 9
11400510 140110000 0 153 1 0.315 10
11400511 140120000 0 153 1 0.335 11
*
11400601 240110000 0 153 1 0.100 1
11400602 240100000 0 153 1 0.120 2
11400603 240090000 0 153 1 0.145 3
11400604 240080000 0 153 1 0.170 4
11400605 240070000 0 153 1 0.195 5
11400606 240060000 0 153 1 0.220 6
11400607 240050000 0 153 1 0.245 7
11400608 240040000 0 153 1 0.265 8
11400609 240030000 0 153 1 0.290 9
11400610 240020000 0 153 1 0.315 10
11400611 240010000 0 153 1 0.335 11
*
11400701 0 0.0 0.0 0.0 11
11400801 0 10.0 10.0 10.0 10.0 0 0 1.0 11
11400901 0 10.0 10.0 10.0 10.0 0 0 1.0 11
*
```

C-5. Simulation for different number of nodes with default model (Simulation : #nd4)

Modification of C-3

1. component 140 and 145

2. component 240 and 270

3. heat structure input

4. simular case : nd1, nd2, nd3

```
* component 140 : condensing tube
* name type
1400000 pipe140 pipe
* nv: no. vol
1400001 18
* area nv
1400101 0.001772 18
* length vn
* ccc0301 - ccc0399
1400301 0.500 1
1400302 0.150 17
1400303 0.400 18
* volume nv
*1400401 0.0 18
* angle vn
1400601 -90.0 18
* rough dhydr no. vol
1400801 1.e-4 0.0 18
* vflag no. vol
1401001 00000 18
* jflag no. jun
1401101 000000 17
* cntrl pressure temp. nv
*ccc1201-ccc1299
1800200 003
1401201 003 0.46546675e6 0.35474181e3 0.0 0.0 0.0 1
1401202 003 0.46546675e6 0.35474181e3 0.0 0.0 0.0 18
* cntrl
1401300 1
* water flow steam flow int.vel jn
1401301 0.0 0.0 0.0 17
*
*
* component 145 : condensing tube to lower plenum
* name type
1450000 sj145 sngljun
* from to area kforw kbackw jflag
1450101 140180002 150010001 0.001772 11.783 7.608
0001000
* cntrl waterflow steamflow x
1450201 1 0.0 0.0 0.0
*
* component 240 : outer tube for coolant water
* name type
2400000 out_tube annulus
* nv
2400001 16
* area nv
2400101 0.005151 16
* length vn
2400301 0.150 16
* volume nv
2400401 0.0 16
* angle nv
2400601 90.0 16
* rough hd nv
2400801 1.e-4 0.0 16
* vflag nv
2401001 00010 16
* jflag nj
2401101 000020 15
* cntrl pressure temp. vn
2401201 003 0.1013e6 0.3024605e3 0.0 0.0 0.0 1
2401202 003 0.1013e6 0.3024605e3 0.0 0.0 0.0 16
```

```
* cntrl
2401300 1
* waterflow steamflow int.vel nj
2401301 0.1514 0.0 0.0 15
*
*
* component 270 : outer tube to coolant outlet
* name type
2700000 sj270 sngljun
* from to area kforw kbackw jflag
2700101 240160002 280000000 0.00049 50.0 90.48
0001000
* cntrl waterflow steamflow x
2700201 1 0.1514 0.0 0.0
*
****************************************
* heat structure input : pipe140 <-> annulus240
* (condensing tube simulation)
****************************************
*
*
* heat structure 140 : heat transfer simulation through pipe
11400000 16 4 2 1 0.02375
11400100 0 1
11400101 3 0.02540
11400201 5 3
11400301 0 3
11400401 373.0 4
*
*11400501 140020000 0 101 1 0.150 1
*11400502 140170000 10000 101 1 0.150 16
*
*11400601 240160000 0 101 1 0.150 1
*11400602 240010000 -10000 101 1 0.150 16
*
*
11400501 140020000 0 101 1 0.150 1
11400502 140030000 0 101 1 0.150 2
11400503 140040000 0 101 1 0.150 3
11400504 140050000 0 101 1 0.150 4
11400505 140060000 0 101 1 0.150 5
11400506 140070000 0 101 1 0.150 6
11400507 140080000 0 101 1 0.150 7
11400508 140090000 0 101 1 0.150 8
11400509 140100000 0 101 1 0.150 9
11400510 140110000 0 101 1 0.150 10
11400511 140120000 0 101 1 0.150 11
11400512 140130000 0 101 1 0.150 12
11400513 140140000 0 101 1 0.150 13
11400514 140150000 0 101 1 0.150 14
11400515 140160000 0 101 1 0.150 15
11400516 140170000 0 101 1 0.150 16
*
11400601 240160000 0 101 1 0.150 1
11400602 240150000 0 101 1 0.150 2
11400603 240140000 0 101 1 0.150 3
11400604 240130000 0 101 1 0.150 4
11400605 240120000 0 101 1 0.150 5
11400606 240110000 0 101 1 0.150 6
11400607 240100000 0 101 1 0.150 7
11400608 240090000 0 101 1 0.150 8
11400609 240080000 0 101 1 0.150 9
11400610 240070000 0 101 1 0.150 10
11400611 240060000 0 101 1 0.150 11
11400612 240050000 0 101 1 0.150 12
11400613 240040000 0 101 1 0.150 13
11400614 240030000 0 101 1 0.150 14
11400615 240020000 0 101 1 0.150 15
11400616 240010000 0 101 1 0.150 16
*
11400701 0 0.0 0.0 0.0 16
11400801 0 10.0 10.0 10.0 10.0 0 0 1.0 16
11400901 0 10.0 10.0 10.0 10.0 0 0 1.0 16
*
```

C-6. Simulation for different number of nodes with alternative model (Simulation : #nd4)

Modification of C-5

1. heat structure input

```
**************************************
* heat structure input : pipe140 <-> annulus240
* (condensing tube simulation)
**************************************
*
*
* heat structure 140 : heat transfer simulation through pipe
11400000 16 4 2 1 0.02375
11400100 0 1
11400101 3 0.02540
11400201 5 3
11400301 0 3
11400401 373.0 4
*
*11400501 140020000 0 153 1 0.150 1
*11400502 140170000 10000 153 1 0.150 16
*
*11400601 240160000 0 153 1 0.150 1
*11400602 240010000 -10000 153 1 0.150 16
*
*
11400501 140020000 0 153 1 0.150 1
11400502 140030000 0 153 1 0.150 2
11400503 140040000 0 153 1 0.150 3
11400504 140050000 0 153 1 0.150 4
11400505 140060000 0 153 1 0.150 5
11400506 140070000 0 153 1 0.150 6
11400507 140080000 0 153 1 0.150 7
11400508 140090000 0 153 1 0.150 8
11400509 140100000 0 153 1 0.150 9
11400510 140110000 0 153 1 0.150 10
11400511 140120000 0 153 1 0.150 11
11400512 140130000 0 153 1 0.150 12
11400513 140140000 0 153 1 0.150 13
11400514 140150000 0 153 1 0.150 14
11400515 140160000 0 153 1 0.150 15
11400516 140170000 0 153 1 0.150 16
*
11400601 240160000 0 153 1 0.150 1
11400602 240150000 0 153 1 0.150 2
11400603 240140000 0 153 1 0.150 3
11400604 240130000 0 153 1 0.150 4
11400605 240120000 0 153 1 0.150 5
11400606 240110000 0 153 1 0.150 6
11400607 240100000 0 153 1 0.150 7
11400608 240090000 0 153 1 0.150 8
11400609 240080000 0 153 1 0.150 9
11400610 240070000 0 153 1 0.150 10
11400611 240060000 0 153 1 0.150 11
11400612 240050000 0 153 1 0.150 12
11400613 240040000 0 153 1 0.150 13
11400614 240030000 0 153 1 0.150 14
11400615 240020000 0 153 1 0.150 15
11400616 240010000 0 153 1 0.150 16
*
11400701 0 0.0 0.0 0.0 16
11400801 0 10.0 10.0 10.0 10.0 0 0 1.0 16
11400901 0 10.0 10.0 10.0 10.0 0 0 1.0 16
*
```

NRC FORM 335 (2-89) NRCM 1102, 3201, 3202

U.S. NUCLEAR REGULATORY COMMISSION

BIBLIOGRAPHIC DATA SHEET

(See instructions on the reverse)

1. REPORT NUMBER (Assigned by NRC, Add Vol., Supp., Rev., and Addendum Numbers, if any.)

NUREG/IA-0147

2. TITLE AND SUBTITLE

Assessment of RELAP5/MOD3.2 for Steam Condensation Experiments in the Presence of Noncondensibles in a Vertical Tube of PCCS

3. DATE REPORT PUBLISHED

MONTH	YEAR
September	1998

4. FIN OR GRANT NUMBER

D6227

5. AUTHOR(S)

H. S. Park, H. C. No/KAIST
Y. S. Bang, K. W. Seul, H. J. Kim/KINS

6. TYPE OF REPORT

7. PERIOD COVERED *(Inclusive Dates)*

8. PERFORMING ORGANIZATION - NAME AND ADDRESS *(If NRC, provide Division, Office or Region, U.S. Nuclear Regulatory Commission, and mailing address; if contractor, provide name and mailing address.)*

Korea Advanced Institute of Science and Technology
373-1 Kuseong-Dong, Yusong-Ku
Taejon, Korea

Korea Institute of Nuclear Safety
P.O. Box 114
Yusong, Taejon
Korea 305-600

9. SPONSORING ORGANIZATION - NAME AND ADDRESS *(If NRC, type "Same as above"; if contractor, provide NRC Division, Office or Region, U.S. Nuclear Regulatory Commission, and mailing address.)*

Division of Systems Technology
Office of Nuclear Regulatory Research
U.S. Nuclear Regulatory Commission
Washington, DC 20555-0001

10. SUPPLEMENTARY NOTES

G. Rhee, NRC Project Manager

11. ABSTRACT *(200 words or less)*

This report deals with the application of RELAP5/MOD3.2 to condensation experiments in the presence of noncondensable gases in a vertical tube of Passive Containment Cooling System. When steam-noncondensable gas mixture was injected into the vertical tube, steam was condensed on the inner surface of the condensing tube but the noncondensable gas greatly inhibited the condensation of the steam. As the scattering of previous experimental data was large, the present experimental appparatus was set up to get reliable data on the condensation heat transfer coefficient of the steam-noncondensable gas mixture in a vertical tube. The experimental results show that the condensation heat transfer coefficient increases as the inlet steam-air mixture flow rate increases, the inlet air mass fraction decreases, and the inlet saturated steam temperature decreases.

There are two wall film condensation models, the default model and the alternative model, in RELAP5/MOD3.2. After a condensation database was constructed, two models were assessed directly with the data of the database. The experimental apparatus was also modeled with RELAP5/MOD3.2, and simulations were performed for several sub-tests to be compared with the experimental results. The simulation results show that in an overall sense the default model of RELAP5/MOD3.2 under-predicts the heat transfer coefficients, but that the alternative model of RELAP5/MOD3.2 over-predicts them throughout the condensing tube.

12. KEY WORDS/DESCRIPTORS *(List words or phrases that will assist researchers in locating the report.)*

steam condensation
condensation inside tubes
non-condensible gas effect
RELAP5/MOD3.2
assessment
passive containment system

13. AVAILABILITY STATEMENT

unlimited

14. SECURITY CLASSIFICATION

(This Page) unclassified

(This Report) unclassified

15. NUMBER OF PAGES

16. PRICE

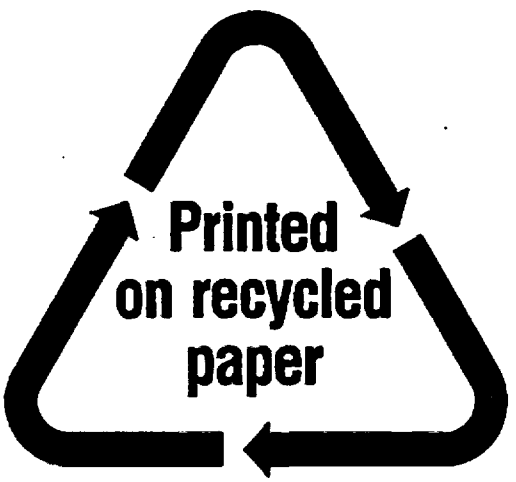

Federal Recycling Program